



Review

Chemical equilibrium analysis of hydrogen production from shale gas using sorption enhanced chemical looping steam reforming



Zainab Ibrahim S G Adiya *, Valerie Dupont, Tariq Mahmud

School of Chemical and Process Engineering (SCAPE), The University of Leeds, Leeds LS2 9JT, UK

ARTICLE INFO

Article history:

Received 21 July 2016

Received in revised form 14 January 2017

Accepted 16 January 2017

Available online xxx

Keywords:

Shale gas

Steam reforming

Chemical looping

Sorption enhancement

ABSTRACT

Detailed chemical equilibrium analysis based on minimisation of Gibbs Energy is conducted to illustrate the benefits of integrating sorption enhancement (SE) and chemical looping (CL) together with the conventional catalytic steam reforming (C-SR) process for hydrogen production from a typical shale gas feedstock. $\text{CaO}_{(s)}$ was chosen as the CO_2 sorbent and Ni/NiO is the oxygen transfer material (OTM) doubling as steam reforming catalyst. Up to 49% and 52% rise in H_2 yield and purity respectively were achieved with SE-CLSR with a lower enthalpy change compared to C-SR at S:C 3 and 800 K. A minimum energy of 159 kJ was required to produce 1 mol of H_2 at S:C 3 and 800 K in C-SR process, this significantly dropped to 34 kJ/mol of produced H_2 in the $\text{CaO}_{(s)}$ /NiO system at same operating condition without regeneration of the sorbent, when the energy of regenerating the sorbent at 1170 K was included, the enthalpy rose to 92 kJ/mol H_2 , i.e., significantly lower than the Ca-free system. The presence of inert bed materials in the reactor bed such as catalyst support or degraded CO_2 sorbent introduced a very substantial heating burden to bring these materials from reforming temperature to sorbent regeneration temperature or to Ni oxidation temperature. The choice of S:C ratio in conditions of excess steam represents a compromise between the higher H_2 yield and purity and lower risk of coking, balanced by the increased enthalpy cost of raising excess steam.

© 2017 Published by Elsevier B.V.

Contents

1. Introduction	129
2. Process description	130
3. Methodology of the thermodynamic equilibrium calculation	132
4. Results and discussion	133
4.1. Effect of temperature and presence of C2–C3 feedstock on both C-SR and SE-SR processes	134
4.2. Effect of steam to carbon ratio on steam reforming processes	134
4.3. Sorption enhancement with CaO sorbent (SE-SR)	135
4.4. Chemical looping with NiO coupled with steam reforming (CL-SR) of shale gas	136
4.5. Sorption enhanced chemical looping steam reforming	138
4.5.1. H_2 yield, H_2 purity and selectivity to carbonate	138
4.5.2. Enthalpy balance of SE-CLSR	138
4.5.3. Effect of inert materials on enthalpy balance of the cyclic processes	140
4.6. Carbon product	140
4.7. Effect of pressure on C-SR and SE-CLSR	142
5. Conclusion and final remarks	142
Acknowledgments	142
Appendix A. Supplementary data	142
References	142

* Corresponding author.

E-mail addresses: pm12zsig@leeds.ac.uk (Z.I. S G Adiya), V.Dupont@leeds.ac.uk (V. Dupont).

1. Introduction

Hydrogen is at present of enormous value in the production of synthetic fertilizers via ammonia manufacture, as well as an essential reagent in petroleum refinery operations [1,2]. Ammonia is the backbone of the fertilizer industry and is generated in industrial processes by reaction between hydrogen and nitrogen at medium temperature and high pressure. Although the use of high pressure in the industrial H₂ production process is detrimental to the equilibrium feedstock conversion and thus of the H₂ yield per mol of feedstock, it permits the utilization of more compact and thus less capital intensive plants. Ammonia production individually represents the largest H₂ consumption, with 50% of all the hydrogen produced in the globe [1–3]. Rapid growth in world population is generating increased demand for food and providing a continued need for agricultural chemicals, especially fertilizers [4]. World-wide ammonia capacity is anticipated to rise 16% (over/in comparison to 2013), reaching 245 Mt NH₃ in 2018 [5]. Hydrogen production, management and recovery within petroleum refineries is also increasing particularly in the production of low-sulphur and diesel fuels using hydrotreating and hydrocracking processes [6,7]. Perhaps hydrogen is the most significant utility in a modern petroleum refinery [8]. As more severe product specifications come into effect, a classic refinery is either 'bottlenecked' due to lack of hydrogen or will be in the future [9]. The increasing stringent requirements on refinery products quality have effect on hydrogen production and demand. Hydrogen at refineries is provided in part by catalytic reforming (main product: cracked fractions, by-product: hydrogen), the remainder being supplied on site or off site by steam reforming (main product: hydrogen, by-product: CO or CO₂), and, to a much smaller extent partial oxidation and autothermal reforming are used [6,9]. Steam reforming can also form the first step in Fischer Tropsch processes, which convert natural gas to gasoline-like liquid fuel [10] via 'GTL' technology. Feedstocks for steam reforming at refineries vary from gases (natural gas 'NG', but also, associated gases, flare gas) to naphtha [11,12]. A boom in shale gas production [13] and unconventional gas resources in the world (e.g. hydrates) foresees that gas will remain the main feedstock of steam reforming in the near term, in contrast to naphtha, which is declining due to high availability of natural gas [13,14]. 'Shale gas is a natural gas found within shale formations' [15] (a form of sedimentary rock). The recent development in oil and gas extraction e.g. drilling and fracking have made shale gas production economically viable. In 2013, the Annual Energy Outlook projected that the U.S (world largest producer of shale gas) natural gas production will increase an estimate of 44% over the next 30 years. Enormous amount of this projected increase is expected from shale gas extraction. Shale gas is also expected to grow from 7.8 million MMcf (million cubic feet) extracted in 2011, to 16.7 million MMcf in 2040. In future, shale gas production in the U.S is anticipated to rise, whereas all other extraction method are likely to remain steady or decline [15,16]. Furthermore, many developed countries have extensive natural gas distribution networks which can act as energy storage and transport facilities with lower losses than their electricity grids, which positions gas as an attractive energy carrier (e.g. UK). The use Natural Gas (NG) fuelled vehicles and NG power stations is also increasing in the world. Gas feedstock compositions are characterised by significant content in hydrocarbons with carbon number 2 to 6, in addition to the main component methane, as well as greatly varying contents in N₂, CO₂, H₂S according to their source [12]. Despite having reached technological maturity, steam reforming is one of the most energy consuming processes in hydrocarbon processing and ammonia production via its heating requirement, with additional disadvantages such as greenhouse gas and other air pollutants emission, high operational and maintenance cost [17].

Researchers are focusing on finding alternative energy efficient technologies that can mitigate the economic and environmental impacts of the forecasted large increases in hydrogen demand. Sorption enhancement (i.e. process with in situ CO₂ capture on a solid sorbent) which

shifts favourably the chemical equilibria of H₂-producing reactions, and chemical looping (i.e. oxygen for oxidative heat is provided by a solid transfer material undergoing redox cycles at medium temperatures), have both drawn attention as promising modifications to the conventional steam reforming process. This is because of their potential for significant energy savings and lower environmental impacts brought about by process intensification features and milder reactive conditions [18]. Addition of 'high temperature' (as opposed to 'flue temperature') solid CO₂ sorbent in the reformer that captures CO₂, shifts the equilibrium of the steam reforming and water gas shift reaction towards maximum hydrogen yield and purity, as well as increasing feedstock conversion [19,20]. Moreover, CO₂ chemisorption is highly exothermic, providing energy directly inside the reformer. Lyon and Cole [21] proposed the coupling of sorption enhancement and chemical looping together for endothermic reactions such as steam reforming, the process first termed 'unmixed' reforming, was later termed 'sorption enhanced chemical looping' steam reforming (SE-CLSR). The process has been studied and analysed using variety of fuels, such as methane [18] and waste cooking oil [22], for hydrogen production using both the interconnected fluidised bed and the fixed bed reactors configurations, which both have their advantages and drawbacks. However, studies on the thermodynamic analysis and process simulation, which are relevant to both types of configurations are limited. Researchers have focused mainly on either the sorption enhanced process [23,24] or the chemical looping process [25] separately. Coupling of sorption enhanced water gas shift and chemical looping with partial oxidation has also been investigated [18]. Moreover, to date, the processes that use typical/actual gas composition containing higher hydrocarbons and inert have not been investigated.

Global warming is presently one of the major concern in the world [26]. The conventional steam reforming (C-SR) process is one of leading causes of global warming; by increasing the CO₂ (the primary greenhouse gas bringing about global warming) concentration in the atmosphere. For every 4 mol of H₂ produced by complete steam methane reforming process for example, a mole of CO₂ is generated. In addition to tons of CO₂ generated and release into the atmosphere by furnace flue gas. SE-CLSR process aimed to overcome this by capturing the CO₂ during the steam reforming process [18,22,27] and eliminating the use of furnace flue gas at steady state operation.

Sorbent degradation is a major concern and drawback on sorption enhanced processes. To make things worse degradation cannot be studied via equilibrium thermodynamics. Researchers worldwide work towards understanding the reasons behind sorbents' loss of CO₂ capacity with repeated cycling and increasing the durability of Ca based CO₂ sorbent [20,28].

In this study, a detailed thermodynamic equilibrium analysis of H₂ production from Marcellus shale gas (see composition in Table 1) using SE-CLSR with CaO_(s) sorbent and NiO as both catalyst and oxygen transfer material (OTM), was conducted. The gas represents a typical composition of natural gas, containing roughly up to 80% of methane with roughly 20% higher hydrocarbons (>C3), CO₂ and inert gas [29], representing a mixture rich in ethane and propane. This composition can also be representative of typical composition of natural gases from Nigeria [30] and the North Sea [31], by containing up to 80% methane [31]. The effect of different input parameters such as temperature,

Table 1
Composition of shale gas used for stimulations [63].

Species	Shale gas (moles)
CH ₄	79.4
C ₂ H ₆	16.1
C ₃ H ₈	4.0
CO ₂	0.1
N ₂	0.4
Total	100

pressure, and molar steam-to-carbon ratio were investigated on the main process outputs of hydrogen yield, purity, feedstock and steam conversion, and carbon formation. The purpose of the study is to demonstrate the effect of coupling SE and CL in C-SR process as well as identify optimum operating conditions of the studied processes using a realistic feedstock. Sorption enhanced reduction of the Nickel oxygen carrier catalyst is also report in the present study for the first time.

2. Process description

Steam methane reforming (SMR) is the most established and commonly used process to produce hydrogen on a large scale [32]. Approximately, 90% of the world's overall hydrogen production is by SMR of fossils fuels [3,32,33]. Fig. 1a depicts a simplified schematic representation of the conventional SMR process henceforth termed 'C-SR'.

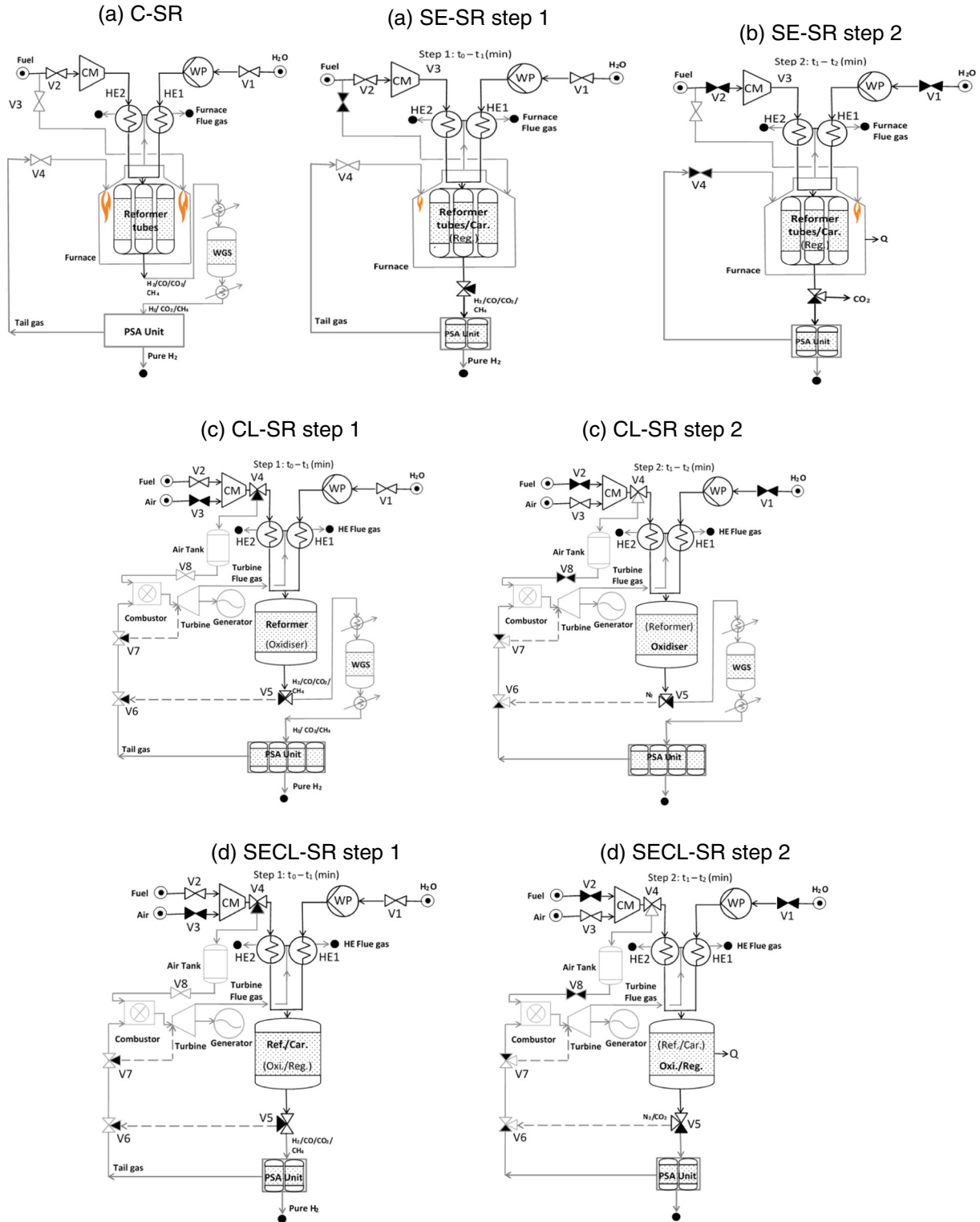


Fig. 1. Schematic description of (a) C-SR, (b) SE-SR steps 1 & 2, (c) CL-SR steps 1 & 2 and (d) SECL-SR steps 1 & 2 processes. CaCO_{3(s)} regeneration occurs during step 2 (highlighted in black, using energy from the exothermic oxidation and gas turbine). Units in grey colour are not covered in our calculation. Blacked out valve symbols (if any) represent closed to flow. Size of flames in furnace are commensurate to heat input from relevant combustible flow (fresh fuel vs. separation unit tail gas).

The process (C-SR), consists of mainly two basic steps followed by separation. In the first stage; water (in the form of high-temperature steam) reacts with feedstock (mainly natural gas) to generate syngas (CO , CO_2 , H_2O , H_2) in the presence of nickel oxide catalyst at an elevated temperature (almost 800–950 °C) and medium pressure (at 20–35 atm) [34,35]. In the second stage, the water gas shift (WGS) reaction runs at a lower temperature (almost 200–400 °C) [36,37]. Although the latter reaction is exothermic, the overall energy demand of the process is significantly endothermic, requiring part of the natural gas to be burnt in the reformer furnace. Separation of the H_2 from the syngas leaving the WGS reactor (mostly unreacted CH_4 , CO , H_2O , and CO_2) is carried out in the final stage. Numerous techniques can be used to undertake separation. Three of the most common techniques used are; pressure swing absorption (PSA), membranes, cryogenics [38,39]. Chemical absorption for example CO_2 scrubbing using methyldiethanolamine (MDEA) and monoethanolamine (MEA) are also used for separation [40]. However, the separation step is not covered in the present thermodynamic analysis. Fig. 1a represents the most common configuration in industrial H_2 production where a PSA unit performs the H_2 separation and the tail gas from the PSA is recycled to the furnace and contributes to meet the reformers heating load.

The purpose of sorption enhanced steam reforming (SE-SR) is to enhance H_2 yield in the conventional steam reforming (C-SR) process [41]. In 1868, H_2 production from hydrocarbon in the presence of $\text{CaO}_{(s)}$ sorbent reportedly took place [18]. A patent for hydrogen production using SE-SR process was issued as early as 1933 [18,42]. As mentioned earlier, the C-SR process route has at least three basic steps; SMR process, WGS and finally the separation/purification step. The logic behind SE-SR process is to perform all those three steps (SMR, WGS and CO_2 capture) simultaneously in a single reactor vessel in the presence of a solid CO_2 sorbent. The role of CO_2 sorbent can be performed cheaply by the abundant calcium oxide or calcium hydroxide [18], but there are other suitable CO_2 sorbents such as hydrotalcites (e.g. $\text{Mg}_6\text{Al}_2(\text{OH})_{16}(\text{CO}_3)_3 \times 4\text{H}_2\text{O}/\text{K}_2\text{CO}_3$) and Li-based sorbents (e.g. Li_4SiO_4). The process is usually configured either using two packed bed reactors operated in cyclic reforming/calcining mode achieved with alternating feed flows, or two fluidised bed reactors with circulating bed materials moving between the reformer (fuel reactor) and the calciner (air reactor). In both cases, the calcination conditions perform the regeneration of the CO_2 sorbent. Although, it is feasible to perform reforming and calcination semi-batch wise in a single reactor vessel, resulting in intermittent H_2 production, a continuous operating process using at least two reactor vessels seems to be more attractive [18]. The CO_2 produced during steam reforming is captured by the sorbent, which once nearly-saturated with CO_2 , is regenerated in situ by temperature or pressure swing adsorption principle. For a Ca-based sorbent, as the CO_2 is been captured $\text{CaCO}_{3(s)}$, the equilibrium of the H_2 -producing reactions is shifted towards the right, increasing hydrogen generation at fairly lower/medium temperatures (723–873 K) compared to the conventional (C-SR) process (1073–1300 K) [18,20,43,44]. Fig. 1b depicts a schematic of the two-step SE-SR process in a packed bed configuration, where step 1 is the H_2 producing step and step 2 the CO_2 sorbent regeneration step. The sorbents play a significant role in the SE-SR process. It is vital for the sorbent to have some certain basic characteristics such as; high selectivity and adsorption ability at operating temperature and pressure, good and steady adsorption capability of CO_2 after repeated adsorption and desorption cycles, and good mechanical strength of adsorbent particles after cyclic exposure to high pressure streams [45, 46]. The most commonly used CO_2 sorbent is CaO [18], which is reduced with CO_2 in an exothermic reaction forming $\text{CaCO}_{3(s)}$ [20]. The carbonated sorbent can be regenerated in order to be useable again by calcination [18,20].

The advantages of SE-SR over C-SR process are; potential to use a lower operating temperature, reduction of purification steps and extent of the reduction, minimisation of reactor size and decrease in the quantity of steam to be used as opposed to C-SR [45,46]. Brun-Tsekhovoi et al.

[47] revealed that the SE-SR process is able to reduce the overall energy required by the system with a potential of saving up to 20–25% as opposed to the C-SR process. In addition to these benefits, the SE-SR process has the advantage of increasing feed conversion, producing high purity hydrogen with a minimum CO_2 , proficient CO_2 capture from the product as $\text{CaCO}_{3(s)}$, and potential to generate pure CO_2 during the sorbent calcination step that is suitable for subsequent use or sequestration [45,46,48]. These advantages are illustrated in Fig. 1b in contrast to Fig. 1a by the absence of WGS stage, a smaller PSA unit, and no large demand of fresh natural gas in the furnace. In the past few years, various SE-SR pilot plants with capacity of 2–20 MW were built in Sweden, Australia, and Germany [49–51]. However, all of the plants used wood chips or woods pellets as fuel for syngas production and the process was demonstrated during gasification [49]. Presently, numerous research groups, both at research institutes and university levels, are investigating the performance of the SE-SR process [41] using various/diverse fuel and feedstocks ranging from methane [24] to propane [23], including hydroxyacetone [52], acetic acid [53], and urea [20].

The chemical looping steam reforming (CL-SR) is a special case which combines chemical looping combustion (CLC) and steam reforming. A metal oxide is used as an intermediate to transport oxygen from air to fuel in order to provide heat of oxidation to the endothermic H_2 production process. This necessitates keeping the air to fuel ratio low to avoid the fuel from been oxidised completely to H_2O and CO_2 [18]. Fig. 1c depicts a schematic of the CL-SR process, step 1 representing the OTM reduction combined with H_2 production, and step 2 corresponding to the oxidation of the OTM.

The process gas is fed into the reactor where both reduction of OTM and steam reforming occur simultaneously. A fraction of the feedstock is expected to be used as reductant in the metal oxide reduction to produce H_2O and CO_2 but the remainder would then reform to CO/CO_2 and H_2 by the catalytically active reduced metal. The second step involves oxidation of the OTM back to its initial state. A best choice of OTM for CL-SR is nickel, as it not only an excellent steam reforming catalyst when reduced by hydrocarbon flow (or NH_3 , or H_2) [54] but is readily oxidised (mainly to NiO) using air, thus an ideal OTM for the CL-SR process. However, the heats of reactions are dependent on oxygen carrier and fuel type [55,56]. The large scale application of CLC and CL-SR is still reliant upon the obtainability of appropriate oxygen carriers. The most commonly studied OTMs are oxides of nickel, copper, iron and manganese. Nickel has been the most used oxygen carrier and considered as state of the art [57,58] because of its high reactivity, negligible volatility, and thermal steadiness which are favourable factors for elevated temperature and high gas turbine CLC [55,56,59,60]. Nevertheless, nickel in particulate form is toxic upon inhalation, and has a thermodynamic constraint of 99–99.5% fuel conversion, conditional on temperature and pressure [58]. Advantages of the CL-SR process over conventional steam reforming are illustrated in Fig. 1c in comparison to Fig. 1a, where the overall surplus energy contained in the syngas and lack of external heating demand in the reformer would in theory permit operating a combustor/gas turbine/electrical generator system. As a result single 'squat' reformer units would be possible that would make the whole plant economical at smaller scales.

The combination of sorption enhancement and CL-SR in one single process and is called sorption enhanced chemical looping steam reforming (SE-CLSR). The material bed then consists of a mixture of particles comprising of solid oxygen carrier and CO_2 sorbent. The reforming reactor normally operates at a low/medium temperature, partially reducing the fuel with the oxygen provided by oxygen carrier and steam reforming most of the fuel, and at the same time any CO_2 produced during the process is captured by the CO_2 sorbent, causing sorption enhanced steam reforming. The overall reaction in the reduction/reforming reactor is thermos-neutral [18,61] owing to the strongly exothermic carbonation reaction. The SE-CLSR process could in principle be self-sufficient with regard to energy because the required heat for the

endothermic steam reforming and reduction reactions could be provided by the exothermic sorbent carbonation reaction, while the heat from re-oxidation of the OTM is utilised for sorbent regeneration [19] in a separate time step. Hence, this could mean near complete elimination of dependency on flue gas use to provide reformer heat at steady state operation. However, full benefits of the process are discussed in detail later. Fig. 1d depicts the SE-CLSR process, with step 1 consisting of the combined OTM reduction, H₂ production under gas and steam flow with in situ CO₂ capture by the sorbent, and step 2 carrying out the coupled OTM oxidation under air flow and CO₂ sorbent calcination. It is suggested that a smaller scale separation process be used, owing to the fact that nearly pure H₂ can be generated in step 1 of the process under well chosen operating conditions. Another capital cost reducing aspect is that instead of needing to use an assembly of many long thin reformer tubes exposed to harsh combustion environments, the reformer could be a single reactor making little use of external heat (e.g. for startup only). The benefits of intensifying the C-SR process by using SE-CLSR technology are pointed out in Fig. 1d in comparison to Fig. 1a, where the furnace and WGS reactor are no longer required, the energy content of the separation gases is used to run (as an example) a combustor/gas turbine-generator, the 'squat' reformer aspect and the reduced separation stage all permit economical downsizing and potentially co-generation.

3. Methodology of the thermodynamic equilibrium calculation

The CEA (Chemical Equilibrium and Applications) software by NASA [62] was used to perform the thermodynamic equilibrium calculations of the gas-water-solid (Ca-based CO₂ sorbent/Ni-OTM) system of four different processes as illustrated in Fig. 1 using a model composition of shale gas as the hydrocarbon feedstock. First, conventional steam reforming (C-SR), then sorption enhanced steam reforming (SE-SR), followed by chemical looping steam reforming (CL-SR) and finally, sorption enhanced chemical looping steam reforming (SE-CLSR) have been simulated. The program uses a solution procedure based on the minimisation of the Gibbs energy function of a feed mixture consisting of hydrocarbon gas, water and solids (Ca-sorbent/Ni-OTM) to calculate the mole fractions of the equilibrium mixture of products. The CEA calculations were conducted at isothermal and isobaric conditions given the endothermicity of the main reaction of steam reforming, permitting changes in volume of the system and representing a reactor mostly necessitating external heat. However, the energy balance of the combined processes will show exothermic balance in some cases, whereby the isothermal conditions would have represented a cooled reactor. Included in the program outputs were specific enthalpy, internal energy, entropy and molar masses of the initial and equilibrium mixtures.

The species considered at equilibrium in the gas-water system in addition to all the gaseous reactants (CH₄, C₂H₆, C₃H₈, N₂, CO₂ and H₂O) were: H₂, CO, C_(s), and NH₃ when simulating the C-SR process. In addition, Ca containing solid species CaO_(s) and Ca(OH)_{2(s)} were included in the reactant mixtures of the sorption enhanced processes (SE-SR and SE-CLSR), with CaCO_{3(s)} as additional product, while NiO_(s) was included in the reactant mixture of the chemical looping processes (CL-SR and SE-CLSR), with Ni_(s) as additional product species. Other related species such as CH₂, CH₃, CH₂OH, C₂H₄, C₂H₅, and CH₃COOH to mention few, were also included in the equilibrium calculations but their molar fractions were <5 × 10⁻⁶ and considered negligible.

The thermodynamic properties (specific heats, enthalpies, entropies) for the initial feed mixture and the equilibrium mixture of products were obtained from NASA [62] and the NIST (National Institute of Standards and Technology) database. The Aspen Plus software's RGibbs model reactor with ideal as well as Peng-Robinson thermodynamic properties were also used for the verification of results. The selected feedstock model composition was based on values found in the literature [63]. A shale gas containing roughly up to 80%

of methane with a significant quantity of higher hydrocarbons (>C₁), CO₂ and inert gas was simulated, representing a mixture rich in ethane and propane. Conditions at equilibrium were provided on the basis of moles of each hydrocarbon gas input (CH₄, C₂H₆, C₃H₈), the molar steam-to-carbon ratio (S:C), the molar calcium-to-carbon ratio (Ca:C), and the molar nickel oxide-to-carbon ratio (NiO:C), as well as system pressure and temperature. The four S:C equilibrium conditions of 0, 1, 2, and 3 were calculated in the study, where 'C' represents 'hydrocarbon' moles of carbon in the gas feed, and 'S' the moles of water feed, as steam. Their choice is justified as follows: S:C of 0 represents the thermal decomposition of the gas. S:C of 1 is the stoichiometric S:C ratio for complete conversion of C_nH_{2n} feedstock to CO and H₂, hence it represents the minimum S:C ratio of practical operation for H₂ generation. S:C of 2 is the condition of stoichiometry for complete conversion of C_nH_{2n} to CO₂ and H₂ formation, while S:C 3 is the condition of excess steam typically used in industrial steam methane reforming, aimed at H₂ production rather than syngas generation [20]. The excess steam also increases the yield and purity of H₂ via Le Chatelier's principle, and in practice inhibits carbon deposition on the catalyst as well as consumes already formed carbon deposits, if any, via steam gasification.

The authors applied their own post processing procedures allowing the calculations of reactants conversions and molar yields of products. A carbon balance was used to facilitate the calculation of the equilibrium total moles produced for the initial mixture chosen ('N_{eq}') and derive products yields and reactants conversions 'X_i' using Eqs. (1.1)–(7). Presentation and discussion of results was based on the following definitions:

$$N_{eq} = \frac{\sum_{i,in} \alpha_i n_{C_i,in}}{\sum_{j,eq} \alpha_j y_{C_j,eq}} \quad (1.1)$$

where n_c represents number of moles of carbon species represented by the subscript indices i in the initial 'in' mixture, and j in the equilibrium 'eq' mixtures. α is the number of carbon atoms in the relevant carbon species. $y_{C_j,eq}$ are the equilibrium mol fraction of carbon containing species j . Henceforth, molar amounts $n_{j,eq}$ obey the equation:

$$n_{j,eq} = y_{j,eq} \times N_{eq} \quad (1.2)$$

where y stands for molar fraction of a particular species in the relevant mixture. Reactants gas and steam conversions (percent or fraction) were defined based on Eqs. (2)–(3)

$$X_{gas}(\%) = 100 \times \frac{\sum_{i,in} \alpha_i n_{C_i,in} - \sum_{i,in} \alpha_i n_{C_i,eq}}{\sum_{i,in} \alpha_i n_{C_i,in}} \quad (2)$$

$$X_{H_2O} = \frac{n_{H_2O,in} - n_{H_2O,eq}}{n_{H_2O,in}} \quad (3)$$

where n is the number of moles of the relevant species (e.g. 'H₂O' is the sum of moles of water) in the relevant conditions (e.g. 'in' or 'eq'). In Eq. (2) subscript i is relevant only to the hydrocarbon species present in the feed mixture.

Two definitions of H₂ yield were used: on mass basis, expressed as % mass of fuel feed (Eq. (4)), and on an absolute molar basis (Eq. (5))

$$H_2 \text{ yield (wt.\%)} = \frac{100 \times 2.02 \left(\frac{g \text{ of } H_2}{mol \text{ of } H_2} \right) \times n_{H_2,eq}}{MW_{gas} \left(\frac{g \text{ of } gas}{mol \text{ of } gas} \right) \times n_{gas \text{ in}}} \quad (4)$$

$$H_2 \text{ yield (mole basis)} = y_{H_2,eq} \times N_{eq} \quad (5)$$

And H₂ purity was defined using Eq. (6).

$$H_2 \text{ purity (dry basis)} = \frac{n_{H_2,eq}}{\sum n_{j,eq}} \times 100 \quad (6)$$

A Ca:C ratio of 1 was used in the SE processes, representing the stoichiometry of the calcium oxide and calcium hydroxide carbonation reactions. The regeneration temperature of 1170 K (~900 °C) was selected to represent temperatures used in practice for decarbonation (calcination) of calcium carbonate in mixtures that may have significant CO₂ content [20,64]. Calculations were made based on the following outputs, where T_R is the reaction temperature:

Carbon products selectivity to CaCO₃:

$$S_{C \text{ to } CaCO_3} = \frac{n_{CaCO_3,eq}}{Tn_{C,eq}} \times 100 \quad (7)$$

The enthalpy balances were performed by summing up the 'reactants' terms to the 'reaction' terms according to the relevant step in the process covered. 'Reactants' term is the enthalpy change of bringing individual reactants from ambient temperature (25 °C) and in their natural phase to a given reaction temperature and potentially new phase (e.g. liquid water to water vapour). A 'Reaction' term is the enthalpy change of conversion to products isothermally at the given reaction temperature for the process step considered. Thermal efficiency of the process is assessed via the 'ΔH ratio' factor. 'ΔH ratio' is the ratio of the total enthalpy change of generating 1 mol of H₂ via the equilibrium steam reforming process under consideration (e.g. C-SR, SE-SR, etc.) to that of generating 1 mol of H₂ via thermal water splitting. Total enthalpy change assumes reactants in their natural state at 298 K (25 °C) and ending with products at reaction temperature. ΔH ratios below the value of 1 showcase a H₂ production process that is thermodynamically advantageous to water splitting. Furthermore, a negative ΔH ratio is obtained for an overall exothermic H₂ production process. Two scenarios were considered in the processes that featured solids: 'A' is used for a total energy balance which does not account for the energy of regeneration of the CO₂ sorbent while 'B' includes the sorbent regeneration energy. The enthalpy terms with the index '1' apply to step 1 of the process considered (fuel and steam feed), and '2' to step 2 (air feed). These terminologies are used in the figures legends and their relevant equations are provided in the supplementary data section.

4. Results and discussion

In this section the effects of nine system conditions on the equilibrium process outputs are discussed, namely: varying temperature, varying S:C ratio, reforming with or without Ca-based CO₂ sorbent, when using CaO, reforming with Nickel Oxygen Transfer Material, reforming with both Ca-based CO₂ sorbent and Ni-OTM, effect of alumina (Al₂O₃) support and degraded sorbent on enthalpy, solid carbon formation and finally pressure. The precise gas composition selected for this study is given in Table 1 and corresponds to Marcellus shale gas (North America). A comparison between C-SR of the shale gas with SE-SR followed by CL-SR and finally SE-CLSR was made to assess the effect on H₂ yield, purity and energy efficiency of the processes, bearing in mind that C-SR of natural gas is at present the industrial standard of H₂ generation. Figures and results at S:C ratio of 3 will be mainly used for illustrations.

The chemical reactions involved in C-SR, SE-SR, CL-SR- and SE-CLSR of shale gas are many and can be summarised by the global reactions R1–R17 (Table 2). Based on the molar inputs of Table 1 for the shale gas/water equilibrium system, the maximum theoretical outputs can be determined according to stoichiometry of the H₂ producing reactions listed in Table 2. Accordingly, the maximum H₂ yield is obtained via the complete reactions R3, R5, R6 (steam reforming of CH₄, C₂H₆ and C₃H₈ respectively) followed by complete R7 (WGS reaction). This would correspond to a H₂ yield of 49.0 wt.% of the shale gas feedstock using Eq. (4). Therefore chemical equilibrium calculations of H₂ yield cannot exceed this value. In the case of H₂ purity, the maximum could be obtained in two ways, the first of which by complete thermal decomposition of CH₄, C₂H₆ and C₃H₈ (e.g. R1), which would achieve a nearly pure H₂ product. This, however, would be to the detriment of the amount of H₂ produced (yield). The second, more desirable way of obtaining a nearly pure gas product would be via complete reactions R3–R7 followed by complete carbonation via R8 or R10, after condensation of water product. The desirable outcomes of the equilibrium calculations are therefore first, a H₂ yield close to the maximum theoretical (stoichiometric) yield, followed by low energy cost, followed last by high H₂ purity. This is because due to stringent purity requirements of some commercial applications, such as in chemicals, pharmaceuticals and petroleum industries, food and beverages industries [2] as well as fuel cell technologies [2,17] a last purification stage may always be needed.

Table 2
Main reactions identified in the gas-water-Ni-Ca equilibrium system.

No.	Reaction	Reaction type
R1	$CH_4 \xrightarrow{Heat} C + 2H_2$	Thermal decomposition
R2	$CH_4 + H_2O \rightleftharpoons CO + 3H_2$	Steam methane reforming →/methanation (hydrogenation) of CO ←
R3	$CH_4 + 2H_2O \rightleftharpoons CO_2 + 4H_2$	Steam methane reforming →/methanation (hydrogenation) of CO ₂ ←
R4	$C_nH_m + nH_2O \rightarrow nCO + (n + 0.5m)H_2$	Hydrocarbon steam reforming
e.g. R5	$C_2H_6 + 2H_2O \rightarrow 2CO + (2 + 3)H_2$	Ethane steam reforming
e.g. R6	$C_3H_8 + 3H_2O \rightarrow 3CO + (3 + 4)H_2$	Propane steam reforming
R7	$CO + H_2O \rightleftharpoons CO_2 + H_2$	Water gas shift (CO-shift) →/reverse water gas shift ←
R8	$CaO_{(s)} + CO_2 \rightleftharpoons CaCO_{3(s)}$	Carbonation of CaO _(s) →/decarbonation or calcination of CaCO _{3(s)} ←
R9	$CaO_{(s)} + H_2O \rightleftharpoons Ca(OH)_{2(s)}$	Hydration of CaO _(s) →/dehydration of Ca(OH) _{2(s)} ←
R10	$Ca(OH)_{2(s)} + CO_2 \rightarrow CaCO_{3(s)} + H_2O$	Carbonation of Ca(OH) _{2(s)}
R11	$C_nH_m + (n)NiO \rightarrow (n)CO + (n)Ni + (0.5m)H_2$	NiO reduction by the fuel, producing CO
R12	$C_nH_m + (2n + 0.5m)NiO \rightarrow nCO_2 + (2n + 0.5m)Ni + (0.5m)H_2O$ E.g. n = 1 and m = 4 for methane	NiO reduction by the fuel, producing CO ₂
R13	$C_nH_m + (n + 0.25m)NiO + (n - 0.25m)H_2O \rightarrow (n + 0.25m)Ni + nCO_2 + (n + 0.25m)H_2$	Combined NiO reduction and global steam reforming reaction of the gas
R14	$Ni + 0.5O_2 \rightarrow NiO$	Ni oxidation to NiO
R15	$C_{(s)} + 2H_2 \rightarrow CH_4$	Carbon hydrogenation
R16	$2CO \rightleftharpoons C_{(s)} + CO_2$	Boudouard reaction (CO disproportionation) →/reverse Boudouard reaction ←
R17	$C_{(s)} + H_2O \rightleftharpoons CO + H_2$	Steam gasification of carbon →

4.1. Effect of temperature and presence of C2-C3 feedstock on both C-SR and SE-SR processes

H₂ yield and purity plots between 500 and 1200 K at S:C ratios of 1, 2, 3, 4, 5 and 6 are displayed in Fig. 2(a and b), respectively. These profiles illustrate a comparative analysis of C-SR and SE-SR of shale gas. In the absence of water (S:C = 0, not shown in Fig. 2), the gas required in excess of 900 K to undergo thermal decomposition and to begin converting significantly to H₂. For S:C of 1, 2, and 3, H₂ yield and purity increased steeply as temperature increased for both the processes. For C-SR, this was caused by conditions shifting from being favourable to methanation (main products CH₄ and CO₂ below 900 K) and other solid carbon forming reactions at a low temperature, to promoting steam methane reforming (main products H₂ and CO₂). This occurred up to roughly 1100 K, where H₂ yield and purity declined and a gentle dwindling in both hydrogen yield and purity was seen with further temperature increase, independent of the S:C ratio, and caused by reverse water gas shift. In the case featuring in situ CO₂ sorption (SE-SR), the H₂ yield and purity profiles with temperature showed a much sharper rise with a wider range of plateau of maximum H₂ yield and purity with temperature, exhibiting the sorption enhancement effects; this is discussed in more detail in Section 4.3. In the low temperature range (<720 K), the presence of C₂ and C₃ species in the reactant gas increases CH₄ yield significantly resulting from the cracking of those species and methanation as further confirmed by the negative CH₄ conversion from 500 to 720 K for C-SR process and from 500 to 540 K for SE-SR process (not shown). The latter resulted from the exothermicity of methanation, favoured at low temperature. Sorption enhancement results in reducing the equilibrium concentration of CH₄ in favour of the process at a higher temperature, thus the higher yield and purity than the conventional processes. Modelling the conditions S:C = 3 with Aspen Plus V8.8 (reactor option RGibbs, properties method Peng Robinson) resulted in an excellent agreement with the results derived from CEA. However, for the SE-SR process a slight difference (decreased in H₂ purity and selectivity of carbon to calcium carbonate) was observed at 1000 K, which might result from the difference in thermodynamic properties of the programmes (ideal in CEA, non-ideal in Aspen Plus). Nonetheless this is relatively insignificant since Ca-sorption enhancement wanes at such high temperature. Similar thermodynamic studies were also conducted with or without Ca sorbent (C-SR and SE-SR process) using several fuels including methane [24], propane [23], hydroxyacetone [52], acetic acid [53], and urea [20]. These results showed a similar trend to those of shale gas (this paper) with regards to H₂ yield and purity and the effect of S:C ratio to be discussed later.

4.2. Effect of steam to carbon ratio on steam reforming processes

For the C-SR process, H₂ yield and purity behaviour with respect to S:C ratio follows Le Chatelier's principle, whereby an increase in the water reactant concentration in the system moves the equilibrium towards higher water conversion, thus causing higher H₂ yield and purity (Fig. 2). However, operating at a large S:C ratio requires higher reactor volume, as well as high operational expenditure for raising steam [20, 23,53]. The effect of S:C ratio levels off at higher values (above S:C 4 and 700–1200 K approximately) [65] as depicted in Fig. 2. The slight increase in the temperature range of 500–700 K in both H₂ yield and purity (above S:C 4) is reasonably insignificant, as industrial steam reforming plant operate around 1073–1273 K roughly [36,37]. Furthermore, using higher S:C ratio is known to cause catalyst and sorbent deactivation because of pore blocking [66,67]. Thus, S:C ratio of 3 typically used in industrial steam methane reforming will be focus on in the presence studies [20]. The curves of H₂ yield and purity against temperature for the varied S:C ratio demonstrate the benefits of operating with high S:C ratio. For example, at 800 K, with the C-SR process case at S:C ratio of 1, the equilibrium H₂ yield is 13.2 wt.% of fuel with 56.0% purity, but it becomes 24.3 wt.% of fuel with 65.4% purity at S:C ratio of 3. This is equivalent to 84% and 17% rises in H₂ yield and H₂ purity, respectively. The higher the S:C ratio, the closer the H₂ yield gets to the theoretical (stoichiometric) maximum of 49.0 wt.%, as well as increasing H₂ purity. The use of high S:C ratio also prevents carbon product (potential deposition on the catalyst) through reaction (R17), however equilibrium carbon is discussed separately in Section 4.6.

Fig. 3(a) depicts the impact of S:C ratio through the value of the ΔH ratio for the C-SR process (2nd y axis). Recall that the furthest ΔH ratio below 1, the more thermally efficient the process is. The profiles in Fig. 3(a) indicate that the ΔH ratio of C-SR penetrated the <1 viability area at similar temperatures of 670 K for S:C ratio of 1, 2, and 3. For S:C ratio of 0 the process was viable at roughly 600 K, representing a process where H₂ is only a minor product, this is confirmed by the growing energy costs of operating at increasing S:C ratio, e.g. minimum ΔH ratio of 0.41 was obtained at stoichiometric S:C ratio of 1 and 800 K, but minimum ΔH ratio became 0.51 at the same temperature at S:C ratio of 3.

The energy balance for molar inputs of shale gas composition in Table 1 is further analysed with the help of Fig. 3 (b) which depicts individual enthalpy terms profiles against temperature. The scales shown on the y axis of Fig. 3 (b) in kJ are not particularly significant because they depend on the molar inputs chosen for the system, however what is significant is the relative positions of each enthalpy term profiles in the figure. The total enthalpy change of the process, and consequently the ΔH ratio, is seen to be dominated by the enthalpy change terms of

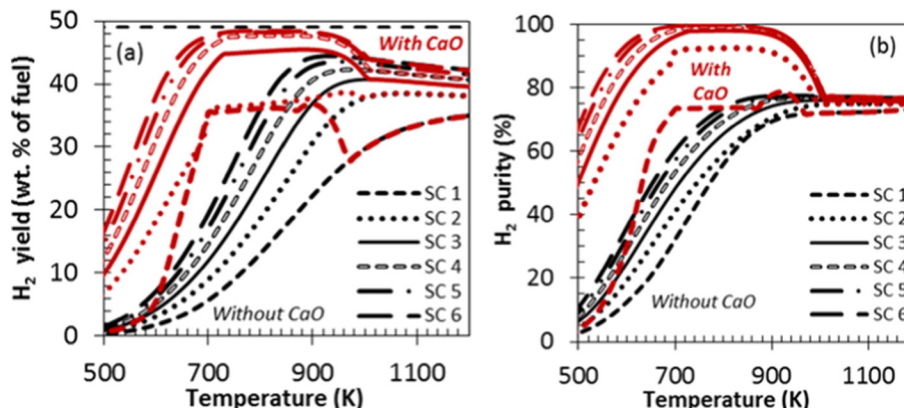


Fig. 2. (a) H₂ yield vs temperature (b) H₂ purity vs temperature at 1 bar, Ca:C 1 and varied S:C ratio (note: the straight line in H₂ yield represent the theoretical maximum).

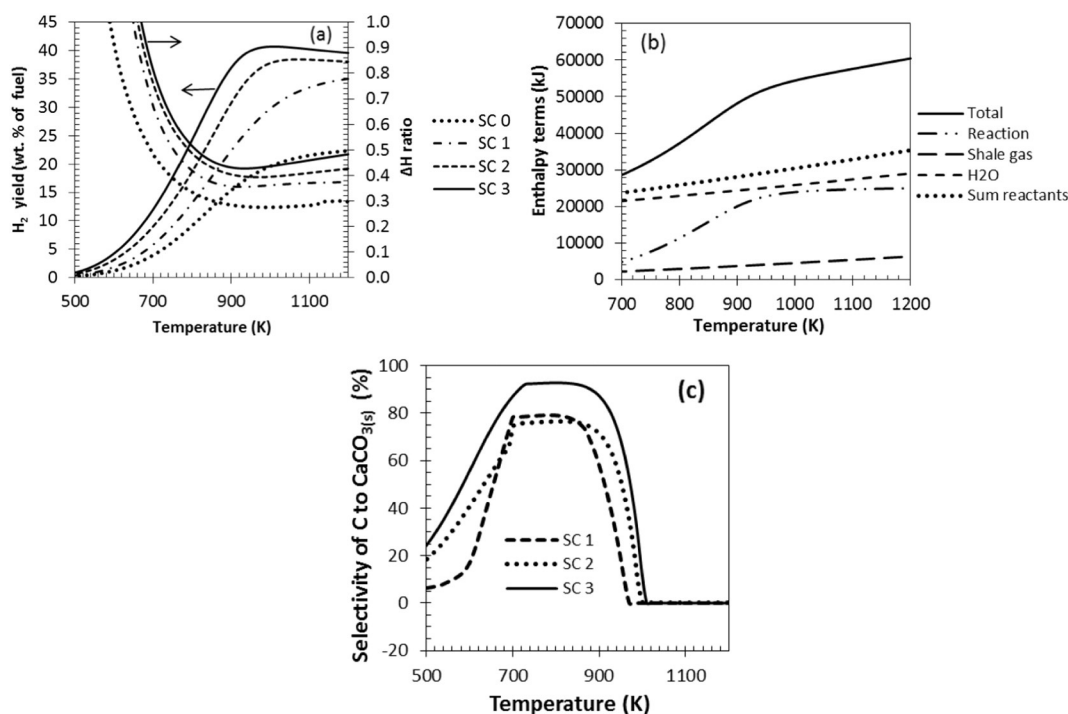


Fig. 3. (a) Effect of S:C ratio on H₂ yield and ΔH ratio vs reaction temperature at 1 bar, without Ca in the system and S:C 0–3 and Table 1 inputs, (b) enthalpy terms vs. temperature for S:C 3 and Table 1 inputs at 1 bar without Ca, (c) selectivity of carbon to calcium carbonate vs temperature at 1 bar, Ca:C 1, and S:C 0–3.

bringing the gas and water reactants to reaction temperature, and in particular that of the water reactant, as opposed to the change in reaction enthalpy. At S:C 1 the total enthalpy change of the process at 800 K and 1070 K were 129 and 118 kJ per mol of H₂ produced, respectively, which further increased to 150 and 130 kJ/mol H₂ at S:C 2, and 159 and 145 kJ/mol H₂ at S:C 3, indicating the increased energy penalty of operating at higher S:C ratios.

4.3. Sorption enhancement with CaO sorbent (SE-SR)

Several benefits of in situ CO₂ sorption are identifiable in the temperature zone of the highest CaCO_{3(s)} yield (500–990 K) on the gas water system at equilibrium. Firstly, H₂ yield increased, bringing it closer to theoretical maximum as depicted by Fig. 2(a). The effects of the CaO_(s) sorbent on the H₂ yield in the low temperature range was brought about by the shift in equilibrium favouring the two H₂ generating reactions (water gas shift and steam reforming), caused by removal of the CO₂ from the syngas product (see diagram Fig. 1(b)). This would have increased both H₂ yield and purity simultaneously as seen in Fig. 2. For instance, the H₂ purity increased from 65.4% without Ca sorbent in the system to 98.0% with CaO_(s) sorbent, at S:C ratio of 3 and temperature of 800 K. This is equivalent to 50.0% rise in purity between the two processes at a steam reforming temperature on the low side, i.e. mild for the solid materials, thus preventing sintering. The latter was accompanied by significant CO and CO₂ reductions with dry mole fractions below 0.01 at 800 K and 0.1 at 1070 K. H₂ yield and efficiency of CO₂ capture is favoured in the low temperature range not only due to thermal decomposition of the sorbent at higher temperatures but also because the equilibrium vapour pressure of CO₂ over CaO_(s) is low at low temperatures [18,19]. Effectively the SE-SR process extends by roughly 110–200 K (depending on S:C ratio in use) the conditions resulting in higher H₂ yield, shifted towards lower temperature, as depicted by Fig. 2(a).

Two regions of temperature were observed in the trends of the process, that result from the sudden drops of Ca(OH)_{2(s)} and CaCO_{3(s)} product yield to zero. This was expected because at temperatures higher

than 700 K, thermal decomposition of Ca(OH)_{2(s)} occurs, while that of CaCO_{3(s)} happens at temperatures higher than 1000 K (Fig. 3(c)).

In addition, the presence of CaO_(s) lowered the energy demand of H₂ generation from the gas-water system. This can be seen in the ΔH ratio farther from 1 for the system with CaO compared to the system without CaO, as shown in Fig. 4(a), due to the lower total change in enthalpy obtained with CaO (Fig. 4b).

Another benefit is reduced energy demand, as shown by the ΔH ratio notably below that of the sorbent-free system, even when accounting for regeneration of the CaCO_{3(s)} back to CaO_(s) through a decarbonation step conducted at 1170 K, as represented by case 'B' (Fig. 4). Sorbent carbonation was reduced at S:C ratio of 0 and 1 due to low carbonate produced. Thus, the effect of sorption enhancement is not properly active at those conditions. For S:C of 2 and 3 the SE-SR process was overall moderately endothermic without sorbent regeneration (case A), but became overall significantly endothermic when accounting for the regeneration step of the sorbent (case B). Regeneration enthalpy change dropped to zero above 1000 K for all the S:C ratios considered due to thermal decomposition of CaCO_{3(s)}, and as a result, the ΔH ratio vs. temperature profiles of the C-SR and SE-SR processes (with and without regeneration) merged with each other, making the later equivalent to the typical C-SR process. The heating cost of the gas was the same for the four S:C ratios (0, 1, 2, and 3) as their molar input remained unchanged. The enthalpy change of raising steam increased with S:C ratio as expected. The energy of heating up the water further confirms the growing cost of operating at a high S:C ratio. The enthalpies of evaporating water and superheating steam at the reaction temperature still dominated the energy balance of the process with sorption enhancement as well. The reaction enthalpy is the backbone of the major difference seen between the two processes (C-SR and SE-SR), illustrated in the ΔH ratios as depicted by Fig. 4(c). This no doubt can be accredited to the carbonation process which is strongly exothermic.

To illustrate the energy savings brought about by in situ CO₂ sorption using CaO_(s) sorbent, the case of S:C ratio of 3 is used. The minimum energy required to bring the system at equilibrium, starting from feed materials of the gas and liquid water at 298 K, was 159 kJ per mol of produced H₂ at 800 K without CaO_(s) in the system. This decreased to

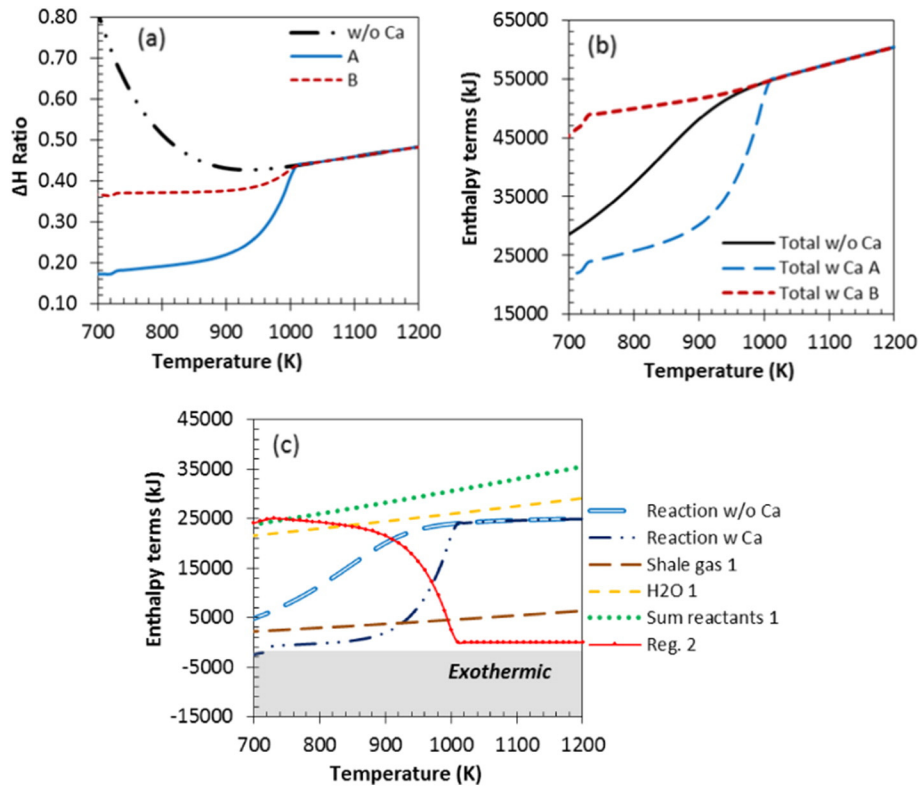


Fig. 4. (a) ΔH ratio vs temperature at 1 bar, Ca:C 1, and S:C 3 (b) total enthalpy terms vs. temperature at 1 bar, Ca:C 1, and S:C 3 (c) enthalpy terms vs. temperature at 1 bar, Ca:C 1, and S:C 3 (note: A and B mean without regeneration and with regeneration respectively while the number 1 and 2 denotes reaction process relevant to step 1 and step 2 respectively).

59 kJ/mol H_2 with $CaO_{(s)}$ without regeneration of the $CaCO_{3(s)}$ (i.e. almost isenthalpic). When including the enthalpy of $CaCO_{3(s)}$ regeneration back to $CaO_{(s)}$ performed at 1170 K, the total enthalpy change rose to 114 kJ per mol of produced H_2 at 800 K respectively, i.e. significantly lower than the sorbent-free system. It is noteworthy that the H_2 producing step (step 1) would be physically separate from the sorbent regeneration step (step 2), and thus during the H_2 production, near autothermal conditions would be reached in step 1 of the SE-SR process.

Accounting for $Ca(OH)_{2(s)}$ and $CaCO_{3(s)}$ as possible products of $CaO_{(s)}$ conversion had different effects on process outputs depending on the S:C ratio and temperature. In situ CO_2 capture by $CaO_{(s)}$ (R8) and hydration reaction of CaO to produce $Ca(OH)_{2(s)}$ (R9) are active at low to intermediate temperatures (<700 K) and the latter competes with both steam reforming and water gas shift reactions for water usage. At temperature of maximum H_2 yield, 800 K approximately, removal of water by CaO was insignificant because thermal decomposition of $Ca(OH)_{2(s)}$ occurred at around the same temperature. Hence $CaO_{(s)}$ was permitted to transform to $CaCO_{3(s)}$ producing the desired sorption enhancement.

4.4. Chemical looping with NiO coupled with steam reforming (CL-SR) of shale gas

Fig. 5 summarises the outputs of steam reforming of shale gas when coupled with chemical looping (CL-SR) using NiO as the oxygen transfer material. For the purpose of comparison of processes, the outputs of C-SR are also included in the figure. The process was investigated by first varying the NiO:C ratio while maintaining S:C of 3 in Fig. 5 (a and b), then followed by changing the S:C between 0 and 3 while maintaining NiO:C 1.0 constant, as depicted in Fig. 5 (c and d).

In the CL-SR process, complete conversion of the gas and good selectivity towards the desired products was achieved. NiO reduction with

the fuel is thermodynamically possible at temperatures as low as 400 K, as indicated by negative water conversion below 400 K. Increasing the NiO:C ratio decreases monotonically the H_2 yield and purity (Fig. 5a). The decrease in H_2 yield can be attributed to CL-processes using part of the fuel according to either R11 (co products CO and H_2) or R12 (co-products CO_2 and H_2O) to meet the energy demand of steam reforming, a role that is normally played by the gas fired furnace in the C-SR process (see Fig. 1a). H_2 purity also decreases with growing NiO:C ratio. This can be explained by concurrent CO_2 generation via the NiO reduction reaction (R12).

One significant benefit of coupling C-SR with chemical looping is the reduced energy demand of the overall H_2 production. This is evidenced by the ΔH ratio notably below that of the NiO-free system (Fig. 6). The reduced energy demand can be attributed to the strongly exothermic nickel oxidation process (one of the major difference between the CL-SR and C-SR process) as shown in Fig. 6(b). The ΔH ratio of the CL-SR process (steps 1&2) was fairly endothermic at low/medium temperature (700–850 K) but slightly decreases at higher temperatures (850–1200 K) with increase in operating temperature. The overall energy demand of the process decrease with increase in NiO:C ratio, making the process almost autothermal at the highest NiO:C ratio (1.0). However, even at the lowest NiO:C ratio energy demand of the CL-SR process was still significantly lower than that of the conventional process (see table SD4 in the supplementary data for ΔH total and ΔH ratio values with varying NiO:C ratios). As expected, the ΔH ratio increased with increasing S:C (0–3) due to the accrued cost of raising the excess steam, as explained earlier (figure not shown). This confirmed that the CL-SR process was also dominated by the cost of raising excess steam (S:C ratio in use). The energy demand of the whole process was dominated in the order of contributions of the following enthalpy terms: sum heating up reactants > sum reactions 1 & 2 as depicted in Fig. 6(b and c). The energy demand of heating up the reactants was in

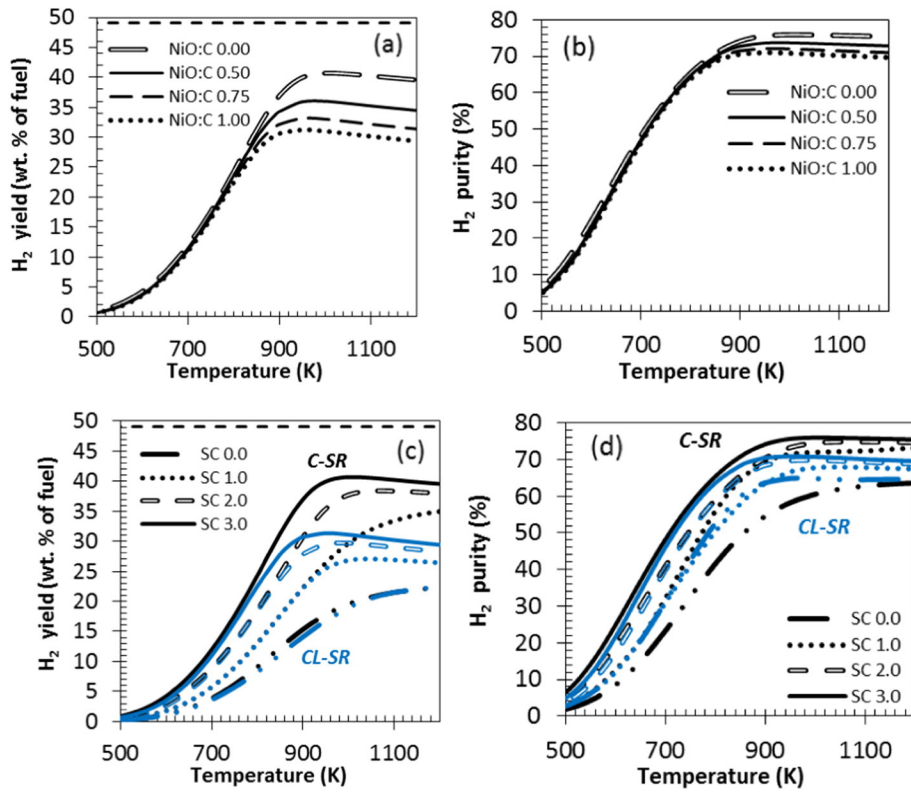


Fig. 5. (a) H₂ yield vs temperature at 1 bar, S:C 3 and varied NiO:C (0.5–1.0) (b) H₂ purity vs temperature at 1 bar, S:C 3 and varied NiO:C (0.5–1.0) (c) H₂ yield vs temperature at 1 bar, NiO:C of 1.0 and varied S:C (0–3) (d) H₂ purity vs temperature at 1 bar, NiO:C of 1.0 and varied S:C (0–3) (note: NiO:C 0.0 denote C-SR process and the straight line in H₂ yield represents the theoretical maximum).

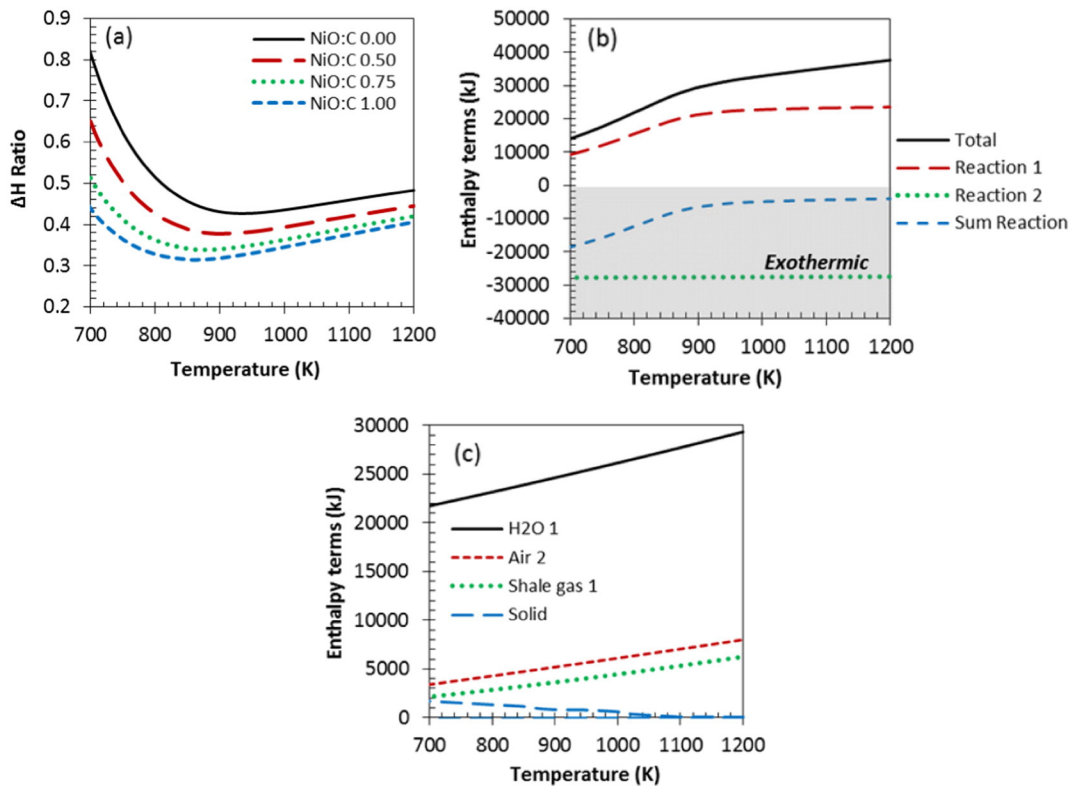


Fig. 6. (a) ΔH ratio of CL-SR vs. temperature at 1 bar, S:C 3 and NiO:C 0.0–1.0 (b) reaction enthalpy terms and (c) sensible enthalpy terms (gases: 298 K → T(K) under stage 1, solid: T(K) → 1100 K under stage 2) vs. temperature at 1 bar, S:C 3 and NiO:C 1.0 (note: the numbers 1 and 2 denote reaction processes stages 1 (reductive & reforming under fuel and steam feed) and 2 (oxidative under air feed) respectively). Temperature T(K) refers to reforming temperature. (Oxidation temperature is assumed to be 1100 K in all CL-SR cases).

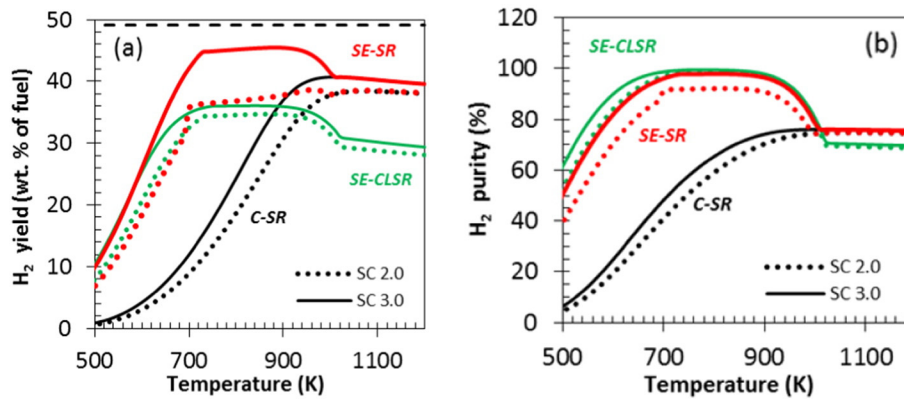


Fig. 7. (a) H_2 yield vs temperature with $CaO_{(s)}$ sorbent at 1 bar, Ca:C 1, NiO:C 1.0 and S:C 2 and 3 and (b) H_2 purity vs temperature with $CaO_{(s)}$ sorbent at 1 bar, Ca:C 1, NiO:C 1.0 and S:C 2 and 3 (note: the straight line in H_2 yield represent the theoretical maximum).

the order $H_2O > air > shale$ gas. The cost of heating up the gas was relatively insignificant compared to those of raising steam from liquid water feed and preheating air.

4.5. Sorption enhanced chemical looping steam reforming

4.5.1. H_2 yield, H_2 purity and selectivity to carbonate

The effect of temperature on H_2 yield and purity is illustrated in Fig. 7 for the three processes (C-SR, SE-SR and SE-CLSR) in the particular case of Ni:C 1.0 and the two S:C of 2 and 3. Note that in the chemical looping processes CL-SR and SE-CLSR, some feedstock is consumed for NiO reduction according to R11 and R12, while for C-SR and SE-SR the fuel is fully available for the steam reforming process. The figure clearly portrays the significance of coupling sorption enhancement and chemical looping in steam reforming with both the superior H_2 yield ca. 700–850 K and H_2 purity ca. 700–1000 K obtained for SE-CLSR compared to the C-SR process (i.e. region of maximum CO_2 capture/efficient carbonation reaction). The presence of the CO_2 sorbent shifts the thermodynamic equilibria of both the steam reforming and the water gas shift reaction (R2 and R7) towards higher conversion to CO, then to CO_2 , followed by capture of the CO_2 on the sorbent, with the carbon product becoming almost exclusively solid calcium carbonate. Subsequently, the presence of the nickel based OTM in SE-CLSR led to even greater H_2 yield (in region of effective carbonation) than C-SR, although part of the fuel was used for reduction. This is because the reduction of fuel by NiO (R12) produces total oxidation products CO_2 and H_2O , with the former being captured by the sorbent, and the latter increasing the water concentration of the system, effectively achieving a double or synergetic enhancement effect. The effect of coupling between C-SR and SE-SR on the H_2 purity in the low/medium temperature zone is explained by the efficiency of CO_2 capture by the Ca sorbent. At high temperatures (roughly above 1000 K), the efficiency of CO_2 capture declined rapidly and dropped to zero, hence the SE-SR process reverted back to C-SR, as conditions favoured $CaCO_3$ decomposition [18,19]. Regarding H_2 purity in the high temperature zone (above 1000 K), the inferiority of SE-CLSR process compared to C-SR and SE-SR was due to the additional CO_2

Table 3
Equilibrium outputs comparing C-SR and SE-CLSR at 800 K Ca:C 1, NiO:C 1.0 and S:C of 2 and 3.

S:C ratio	Conditions	H_2 yield (wt.% of available fuel)	H_2 purity (%)	Selectivity of C to $CaCO_{3(s)}$ (%)
2	Without Ca	19.0	59.2	n/a
2	With CaO & NiO	35.0	98.5	96.1
3	Without Ca	24.3	65.4	n/a
3	With CaO & NiO	36.1	99.5	99.0

present at equilibrium resulting from the NiO reduction, while C-SR and SE-SR performed equally due to decomposition of the $CaCO_{3(s)}$. On the other hand, the inferiority of the process (SE-CLSR) compared to SE-SR with regards to H_2 yield was due to the fact that part of fuel was used for NiO reduction while the fuel was completely available for steam reforming in the case of SE-SR process [68].

Therefore the optimal operating temperatures for both SE-SR and SE-CLSR at atmospheric pressure were around 700–850 K approximately, as illustrated in Fig. 7.

In practice, when using packed bed configuration used with alternating feed flows, it is envisaged that at least two packed bed reactors would be used in parallel, one undergoing the reductive stage with in situ CO_2 capture while the other is in oxidative stage with sorbent regeneration (and potentially carbon burn off), as shown in Fig. 1(d). Table 3 compares the equilibrium outputs of C-SR and SE-CLSR process using CaO as the CO_2 sorbents at 800 K.

Fig. 8 depicts the selectivity of carbon products to $CaCO_{3(s)}$ as a function of temperature for the SE-SR and the SE-CLSR processes. SE-CLSR offers higher selectivity to the carbonate product for a wider range of temperature over SE-SR with CaO. This is because the reduction process increased the water concentration in the system, in favour of CO_2 formation, hence allowing the maximum sorption. At temperatures above 1000 K the efficiency of the CO_2 capture declined because of the favoured carbonate decomposition [18,19].

4.5.2. Enthalpy balance of SE-CLSR

Significantly reduced energy demand was seen in the SE-CLSR process as depicted in Fig. 9, notably below those of both the C-SR

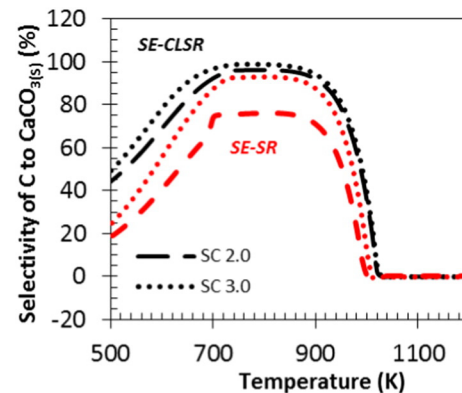


Fig. 8. Selectivity of carbon to calcium carbonate vs temperature at 1 bar, Ca:C 1, NiO:C 1.0 and S:C 2 and 3 with $CaO_{(s)}$ sorbent.

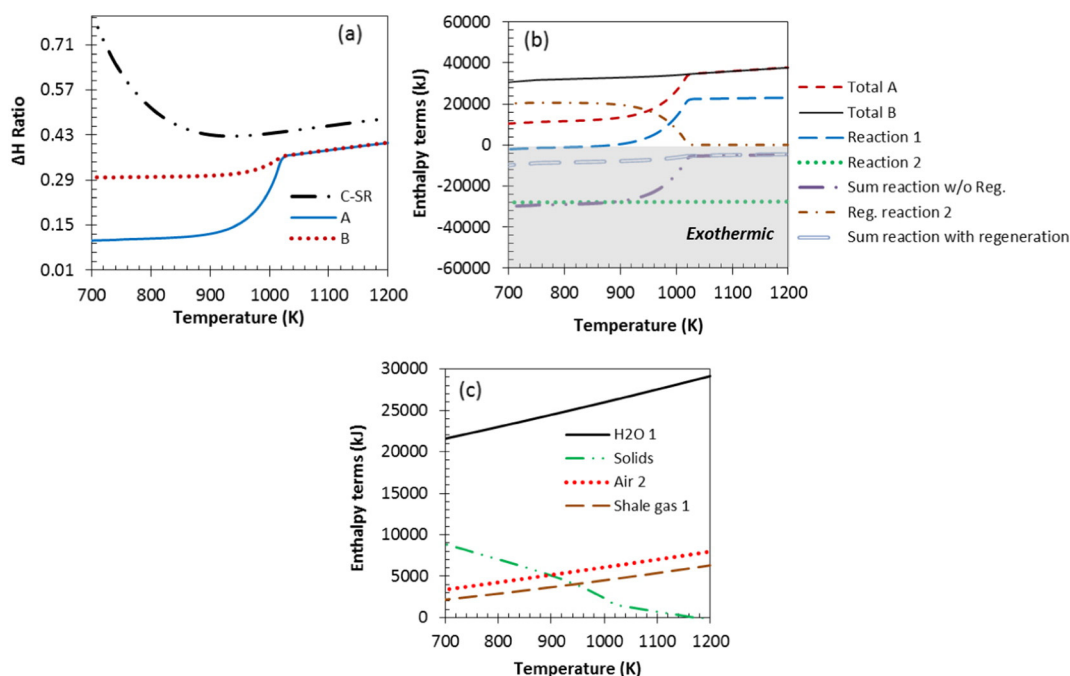


Fig. 9. ΔH ratio and enthalpy terms vs. reforming temperature for SE-CLSR at 1 bar, Ca:C 1, NiO:C 1.0 and S:C 3 (a) ΔH ratio vs. reforming temperature (b) total enthalpy terms vs. reforming temperature (c) sensible enthalpy terms vs. reforming temperature (note: A and B mean without and with $\text{CaCO}_{3(s)}$ regeneration to $\text{CaO}_{(s)}$ at 1170 K, respectively, while the numbers 1 and 2 denote reaction process stages 1 (reductive/reforming) and 2 (oxidative/regenerating) respectively at 1170 K).

and SE-SR process, even when accounting for complete regeneration of the $\text{CaCO}_{3(s)}$ back to $\text{CaO}_{(s)}$ via a decarbonation step conducted at 1170 K. The ΔH ratio without regeneration was slightly endothermic (overall autothermal process) at low/medium temperature range (700–900 K) for S:C 2 but moderately endothermic (almost autothermal process) at S:C 3 with $\text{CaO}_{(s)}$ sorbent. When the enthalpy of regenerating the $\text{CaO}_{(s)}$ sorbent at 1170 K was included, the ΔH ratios became significantly endothermic (positive) but remained significantly lower than the C-SR process, thus more energetically favourable. The heating demand of the gas and air was the same for the S:C 2 and 3 as their molar input remained unchanged. On the other hand, the heating demand of water increased with increase in S:C ratio (discussed earlier) i.e. S:C 2 < S:C 3. Although steam reforming and NiO reduction are endothermic processes, the total reaction enthalpy of the two-step cyclic process (stage 1 + stage 2) was overall exothermic, with the exothermicity decreasing with increase in stage 1 reaction temperature. We chose to show how this excess energy could be used by including a combustor/gas turbine/generator system in Fig. 1(d), as it is the most flexible way to utilise the enthalpy of combustible as well as non-combustible streams via by-passing the combustor. The overall exothermicity resulted from the strongly exothermic Ni oxidation process, as shown in Fig. 9. Both Ni oxidation and carbonation reactions have significantly lowered the energy demand of the hydrogen production. The ΔH ratio of the two processes (C-SR and SE-CLSR) did not merge when decarbonation process stopped (at roughly 1000 K) like the SE-SR process, this effect can be explained by the activity of chemical looping and no doubt can be accredited to the strongly exothermic nickel oxidation. The total energy cost of the process was, again, dominated by water enthalpy change followed by the reaction enthalpy (Fig. 9(c)).

The results of the chemical looping processes (CL-SR and SE-CLSR) were further verified by the authors with Aspen plus 'RGibbs' reactor modelling and were in good agreement to those of CEA. Previous studies were conducted on CL-SR process by [25] and SE-CLSR process by [18, 19, 65, 69]. The results are in good agreement to those of the present study with regards to H_2 yield and purity, selectivity of carbon to calcium carbonates (SE-CLSR process only) as well as reduced energy requirement of the processes when compared to the conventional

process. Optimum operating conditions for SE-CLSR also happen to be in the same range to those reported in the present study 700–850 K, 1–4 bar pressure, S:C 3 and Ca:C 0.8–1 [19]. Zhu and Fan, 2015 [69] analysed the influence of Ca:M ratio, M(fuel):M ratio and Ni:M ratio on SE-CLSR process using equilibrium calculations, they found Ca:M = 1, M(fuel):M of 0.2 and Ni:M of 0.8 were optimum operating condition. Their conclusion (production of high purity hydrogen in the lower operating temperature range compared to CL-SR process) is in good agreement with the present study. Fan and Zhu, 2015 [70] investigated the performance of a novel polygeneration system driven by methane aimed at producing high-purity H_2 through chemical looping combustion thermally coupled with CaO sorption enhanced methane steam reforming (they termed it CLC-SEMSR) combined with power generation through combined cycle. They stimulated the process using Aspen Plus exiting functions and build in functions. They found that the novel polygeneration system can achieve higher exergy efficiency of 83.1% compared to 68.7% in the C-SR process. Their conclusion that polygeneration systems for H_2 production and power generation simplifies the overall process with a more reasonable utilization of fuel, in addition to CLC-SEMSR process potential to produce higher H_2 yield and purity with reduced energy consumption for CO_2 separation is in good agreement with the present study. However, all of the thermodynamic studies (on SE-CLSR process) focussed pure methane as fuel in previous literature and most of the previous studies such as [69, 70] used fluidised bed reactor (air and fuel reactor separate). Researchers also investigated the performance of Ca-supported sorbent on the SE-CLSR process. For example, Fernandez et al. [71], modelled the SE-CLSR process using a Ni based (9% on Al_2O_3 support) OTM/catalyst and a Ca/Cu sorbent with pure methane feedstock. They investigated the effect of catalyst/sorbent ratio, space velocity, S:C ratio, temperature and pressure. They found the optimum operating condition in the temperature range of 923–1023 K, at low-medium pressures (5–15 bar) and high S:C ratio of 3–6. The differences in the optimum operating condition with the present study could be attributed to differences in operating conditions, model used for stimulation and most likely differences in CO_2 sorbent used in addition to the fact that temperatures lower than 873 K were not investigated. Martínez et al. [72] performed a detailed

Table 4

Equilibrium outputs at 800 K (ΔH total and ΔH ratio at 1 bar, Ca:C 1, NiO:C 1.0, and S:C 2 and 3. A and B mean without sorbent regeneration and with sorbent regeneration respectively).

Conditions	ΔH total (kJ/mol H ₂)	ΔH ratio
C-SR S:C 2	150	0.49
SE-CLSR S:C 2 With CaO A	12	0.04
SE-CLSR S:C 2 With CaO B	71	0.23
C-SR S:C 3	159	0.51
SE-CLSR S:C 3 With CaO A	34	0.11
SE-CLSR S:C 3 With CaO B	92	0.30

and complete process design of a H₂ generation plant using natural gas as feedstock, Ni based OTM/catalyst and a novel Ca/Cu CO₂ sorbent as well. Their findings, compact design and the use of cheaper materials compared to C-SR process is in good agreement with the present study (Table 4).

4.5.3. Effect of inert materials on enthalpy balance of the cyclic processes

The presence of inert solid materials in the reactor bed does not affect the equilibrium materials balances (i.e. H₂ yield and purity are the same with inert materials compared to without inert materials), as they do not affect the gas phase equilibrium reactions. However, inert materials would require heating or cooling as required during the cycles of the CL processes. There are two types of inert materials that may be present at any time in the reactor: the oxygen transfer catalyst support, and the degraded CO₂ sorbent material. During cyclic operation, the bed materials require heating from reaction temperature to regeneration temperature (SE-SR with regeneration, and SE-CLSR) or to oxidation temperature (CL-SR), and the active part of the sorbent undergoes decarbonation during regeneration. In the SE-CLSR process, Ni oxidation and decarbonation reactions occur together at sorbent regeneration temperature, 1170 K. In the following section, the individual effects of catalyst support and of degraded sorbent on the total enthalpy change of the cyclic processes are discussed.

4.5.3.1. Oxygen transfer catalyst support. In practice, oxygen transfer materials as well as solid phase catalysts are structured so that a significant part of the material does not participate in the reactions (or it does in a minimal way), but imparts desirable properties to the reactor bed, e.g. morphological (high surface area), mechanical (strength) and thermal (phase stability), so they act as ‘support’ to the chemically active component [56]. Thus NiO is not used on its own in the reactor, but as part of NiO on a support. To represent this effect on the enthalpy balance, an 18 wt.% NiO on α -Al₂O₃ support (typical commercial steam reforming catalyst) [73] was simulated for the CL-SR and the SE-CLSR processes (Fig. 10). This introduced α -Al₂O₃ (corundum) as an additional ‘inert reactant’ in the molar ratio of Al₂O₃: NiO of 3.34, and the cases are described as either ‘with support’ or ‘without support’. Typically it was found that a cyclic process with support in proportions of

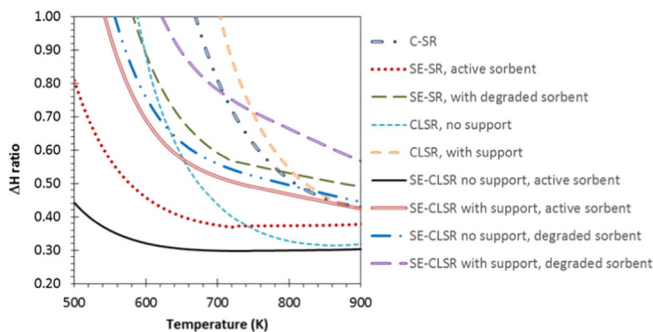


Fig. 10. SE-CLSR: process 2 at 1170 K, active Ca:C = 1, CL-SR: process 2 at 1100 K, S:C = 3, NiO:C = 1, “no support”: NiO 100 wt.%, “with support”: 18 wt.% NiO/Al₂O₃, “active sorbent”: 100% CaO, “degraded sorbent”: 10% active CaO and 90% inert CaO.

Al₂O₃: NiO of 3.34 saw its ΔH ratio increase by about 0.2 compared to the same process without support, although the gap between the two reduced as reforming temperature increased. For instance, at the reforming temperature of 800 K, CL-SR without support had a ΔH ratio of 0.33 compared to 0.54 with support. For the SE-CLSR, at 800 K, ΔH ratio was 0.30 without support but 0.45 with support. By comparison C-SR at 800 K had a ΔH ratio of 0.51. Here the CL-SR appears at disadvantage compared to the conventional process for reforming temperatures below 840 K, which was caused by the assumption that the nickel oxidation step was carried out at 1100 K. When reducing the oxidation temperature to 1050 K, which is sufficient to completely oxidise carbon black deposits on an 18 wt.% NiO/ α -Al₂O₃ catalyst [74], the ΔH ratios of the CL-SR with support and the C-SR processes were the same at a reforming temperature of 800 K.

This implies that heat recuperation from the solids and gases from the regeneration step, not represented here, could play a crucial role in making the CL-SR viable when using a highly supported catalyst. The incentive is thus to minimise the amount of support required for the bed materials to maintain the right properties.

4.5.3.2. Degraded CO₂ sorbent. Similarly, another potential additional energy cost can be brought about by the deactivation of the CO₂ sorbent. Over many cycles, natural Ca-based sorbents typically stabilise to ca. 8–10% of their ‘fresh’ CO₂ capacity [75]. Sorbent materials such as limestone would then contain 90–92 wt.% of inert sorbent. The latter would also present a sensible enthalpy burden when bringing the bed materials to regeneration temperature (here assumed 1170 K). The effect of degraded sorbent in the bed was represented by introducing in the reactants mix the equivalent of 90 wt.% of the total molar calcium in the feed as inert CaO. The Ca:C ratio of 1 quoted in the figures refers to the active CaO.

The ΔH ratios of the SE processes (SE-SR and SE-CLSR with and w/o support) were seen to also increase by around 0.2 at 800 K for the cases with degraded sorbent compared to the active sorbent, with a narrowing gap as the reforming temperature approached the regeneration temperature of 1170 K. Note that above 880 K, the sorption enhancement gradually disappeared as a result of decarbonation of the sorbent. This meant that, typically for reforming temperatures above 800 K, the SE-SR with 90% degraded sorbent and the SE-CLSR with support and 90% degraded sorbent both became less energetically viable than the conventional C-SR process. For the SE-CLSR process with support and 90% degraded sorbent to become more energetically viable than the C-SR process, reforming temperatures would have to reach 720 K, which is the equilibrium lower limit for sorption enhancement as per Figs. 7 and 8. This would imply the use of a very active steam reforming catalyst. At lower temperatures, energetics would be favourable but selectivity to hydrogen product would drop (lower yield and lower purity).

With regards to environmental aspects; SE-CLSR process could be an effective and eco-friendly way of generating H₂ if the challenges associated with the energy costs of heating the bed materials to regeneration/oxidation temperature were to be addressed. The overall GWP of a C-SR plant is 11,888 g CO₂ equivalent/kg of H₂ from which Hydrogen plant operation only account for 78.8% (8895 g CO₂ equivalent/kg of H₂) [76]. SE-CLSR would also have to address the issues of life cycle analysis brought about by the use, operation lifetime and recyclability of the OTM catalyst and sorbent materials. As the majority of the world’s hydrogen is generated through steam reforming of fossil fuels, there will be no elimination of greenhouse gases till CO₂ is sequestered at the source [77].

4.6. Carbon product

Generally, operating at a high S:C ratio inhibits solid carbon formation, as gasification reactions are promoted. This is one of the reasons steam reforming plants aim to operate with some excess of steam.

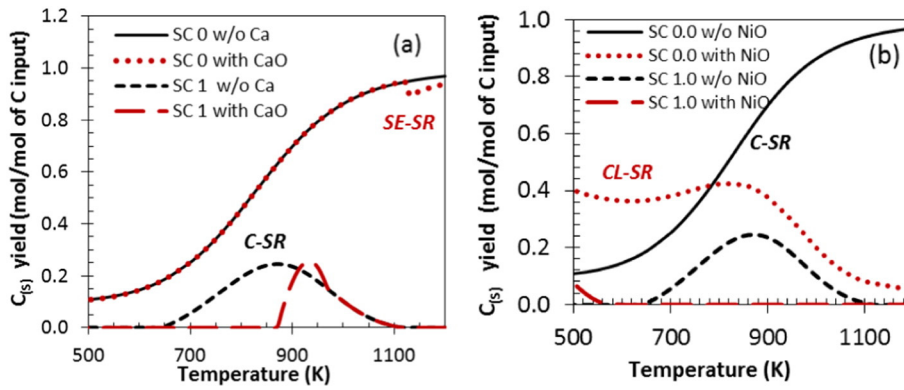


Fig. 11. Carbon yield at 1 bar and S:C 0 and 1, (a) Ca free and Ca sorbent systems, (b) Ca free and CL-SR system at NiO:C 1.0.

Solid carbon in the equilibrium products not only deactivates catalyst by covering its active sites but also reduces H₂ yield and purity because it represents carbon that does not react with steam to generate H₂. Solid carbon product is completely prevented at equilibrium conditions of S:C 2 and 3 in all the processes via steam gasification of carbon (R17) [78]. As shown in Fig. 11, solid carbon product mainly occurs at S:C between 0 and 1, with the quantity of carbon product depending on the process in use. As expected, enormous carbon was generated at S:C ratio of 0 in both the Ca free and CaO_(s) sorbent system. No doubt this resulted from the absence of steam reactant in the system which lowered the amount of CO₂ product to be generated and thus to be adsorbed. Hence, the process behaves like C-SR, consequently the outputs of the SE-SR and C-SR processes at S:C 0 merge with each other. For S:C 1 in the Ca-free and CaO_(s) sorbent system, solid carbon equilibrium product was significantly low (nearly zero) in the low temperature range (500–650 K) but rose in the region of maximum H₂ yield

before exhibiting a gentle dwindling that approaches zero at higher temperatures (1000–1200 K). The sub stoichiometric conditions (limited water in the system) again are the reason behind this observation. As depicted in Fig. 11(b), solid carbon product is significantly low in the CL-SR system compared to C-SR system at same operating conditions. This stems from the fact that water can be a product in the NiO reduction process (R12), thus, favours suppression of equilibrium solid carbon. At S:C 1 in the CL-SR system, solid carbon formation declines gradually and approaches 0 significantly owing to the increase in water concentration in the system as mentioned previously. This further portrayed the positive impacts of operating at super-stoichiometric S:C ratio. In the SE-CLSR process, formation of solid carbon was completely eliminated not only at S:C ratio of 2 and 3 but also at S:C ratio 0 and 1 as well. This no doubt is attributed to effectively achieving sorption enhancement of the NiO reduction reaction, which is identified here for the first time, and the sorption enhanced steam reforming reaction.

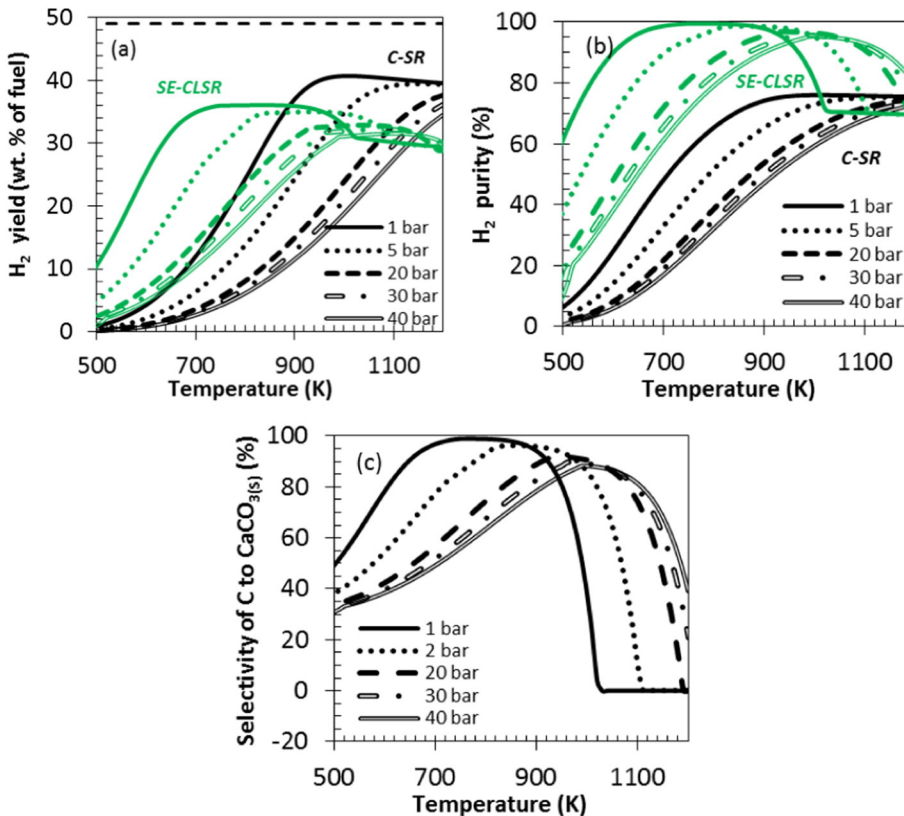


Fig. 12. Effect of pressure at NiO:C 1.0 and S:C 3 (a) H₂ yield vs temperature with CaO sorbent (b) H₂ purity vs temperature with CaO sorbent (c) selectivity of carbon to calcium carbonate vs temperature with CaO sorbent.

4.7. Effect of pressure on C-SR and SE-CLSR

Although steam reforming is affected by pressure negatively in accordance with Le Chatelier's principle due to volumetric increase, it is highly desirable to operate under elevated pressures in industrial plants, which enables higher throughputs, flows over large piping distances, sorption processes, and reduces reactors and gas storage volumes. The effect of pressure on steam reforming is investigated at S:C ratio of 3 because it is the condition of excess steam typically used in industrial steam reforming [20] aimed at hydrogen generation rather than syngas generation. Equilibrium conditions of 1 bar, 5 bars, 20 bars, 30 bars and 40 bars were calculated. Their choice was justified as follow: 1 bar represents atmospheric pressure and typically used for the lab-scale experimental work and derivation of kinetic rates, and a pressure range between 20 and 40 bar represents typical pressure values used in commercial steam reforming operations [79].

The effect of pressure on both the Ca-free system and that with a Ca sorbent in the system follows Le Chatelier's principle. When the pressure was increased to above atmospheric pressure, the H₂ reactions equilibrium shifted to H₂ consumption to a very large extent to counteract product volume expansion, resulting in low H₂ yield and purity as depicted in Fig. 12. H₂ yields of the C-SR and SE-CLSR processes decreased with increase in operating pressure. However, above 900 K, H₂ purity of the SE-CLSR process slightly increased with pressure. This occurred as partial pressure of CO₂ favoured the carbonation reaction leading to higher H₂ purity [80].

In order to increase the partial pressure of CO₂ in the stripping gas the temperature of the adsorption step will always be lower than that of the desorption step. Furthermore, low/medium temperatures limit the maximum partial pressure of CO₂ that can be recuperated from the sorbent. Similarly, it is desirable that regeneration of sorbent (CO₂ desorption) be conducted at as lower total pressure as possible, to increase the quantity of CO₂ desorbed [43,65,81]. Thus, thermal swing is suggested for desorption of the sorbent, as per our assumption of regenerating at 1170 K. Steam is a good carrier gas for CO₂ since it can be easily condensed out of the CO₂ stream before being prepared for sequestration, with potential to minimise the steam usage. Thus, advantageous to the whole system performance [81].

5. Conclusion and final remarks

Using ideal materials properties, represented by an oxygen transfer material little diluted by inert support, and by fully active CO₂ sorbent, sorption enhanced chemical looping steam reforming can have considerable advantages compared to conventional steam reforming for H₂ production because of the substantial increase in H₂ yield and purity, as well as significant drop in temperature of the maximum H₂ yield with effective capture of CO₂ under well-chosen operational conditions. The opportunity of operating the Ca sorbent system at a low temperature could in turn decrease the need to operate at the higher pressure end, thus thermodynamically favouring the H₂ producing reactions. In the ideal bed materials conditions, near full sorption enhancement (over 95% efficiency of CO₂ capture) was observed about 700–900 K and atmospheric pressure, this nearly eliminated the need for further purification steps (CO shift, PSA) as well as expected to minimise the energy cost of operating the system. The energetic cost of shale gas reforming with and without Ca in the system is dominated by the enthalpy change of heating up the liquid water at 298 K and phase transformation to superheated steam at the reaction temperature, depending on S:C ratio in use. The choice of S:C ratio in conditions of excess steam represents a compromise between the higher H₂ yield and purity and low risk of solid carbon formation balanced by the increased energy demand of raising excess steam. The greater the S:C ratio of choice, the greater the enthalpy change of raising the steam will be, and vice versa. Addition of NiO to steam reforming system will decrease the thermal energy requirement of the process. Synergetic enhancement effects

(favourable equilibrium shifts) are observed by the generation of steam from the NiO reduction step, which in turn promotes the steam consuming H₂ production and CO₂ generating reactions while CO₂ is captured, allowing for safe operation (non carbon generating, high H₂ yield) at lower temperatures and lower S:C ratios than the conventional process with excess heat.

Atmospheric pressure and S:C ratio of 3 are found to be optimum for each of the studied processes. Temperature range between 1000 and 1010 K is best for the C-SR process, while 870 to 1000 K temperatures are optimum for CL-SR process. On the other hand the range 700 to 850 K are most beneficial for the SE-SR and SE-CLSR processes. Up to 49% and 52% rise in H₂ yield and purity respectively were achieved with SE-CLSR compared to C-SR at S:C 3 and 800 K. The enthalpy of bringing the system to equilibrium also decreased significantly in the system. A minimum energy of 159 kJ is required to produce 1 mol of H₂ at S:C 3 and 800 K in C-SR process, this significantly drops to 34 kJ/mol of produced H₂ in the CaO_(s)/NiO system at same operating condition without regeneration of the sorbent, but when the energy of regenerating the sorbent at 1170 K was included, the enthalpy rose to 92 kJ/mol H₂. This is still significantly lower than the Ca-free system.

Presence of inert bed materials in the reactor bed such as catalyst support or degraded CO₂ sorbent introduce a very substantial heating burden to bring these materials from reforming temperature to sorbent regeneration temperature or to Ni oxidation temperature, if different. Motivation for future research in the SE-CLSR process ought to focus on these two issues in order to maintain the theoretical advantages of SE-CLSR over the conventional steam reforming process.

Acknowledgments

The Petroleum Technology Development Fund (Nigeria) is gratefully acknowledged for the scholarship of Zainab Ibrahim S. G. Adiya, and we also thank the UKCCSRC EPSRC consortium (EP/K000446/1) for call 2 grant 'Novel Materials and Reforming Process Route for the Production of Ready-Separated CO₂/N₂/H₂ from Natural Gas Feedstocks'.

Appendix A. Supplementary data

Supplementary data to this article can be found online at <http://dx.doi.org/10.1016/j.fuproc.2017.01.026>.

References

- [1] D.P. Harrison, Z. Peng, Low-carbon monoxide hydrogen by sorption enhanced reaction, *Int. J. Chem. React. Eng.* 1 (2003) 1542–6580.
- [2] R. Ramachandran, R.K. Menon, An overview of industrial uses of hydrogen, *Int. J. Hydrog. Energy* 23 (1998) 593–598.
- [3] F.-X. Chiron, G.S. Patience, S. Riffart, Hydrogen production through chemical looping using NiO/NiAl₂O₄ as oxygen carrier, *Chem. Eng. Sci.* 66 (2011) 6324–6330.
- [4] Anon, Ammonia global market to 2020 - food security concerns driving demand for ammonia-based fertilizers, Research and Markets, <http://www.prnewswire.com/news-releases/ammonia-global-market-to-2020-food-security-concerns-driving-demand-for-ammonia-based-fertilizers-216913621.html> 2014 (accessed 09.03.15).
- [5] P. Heffer, M. Prud'homme, Fertiliser Outlook 2013–2018, International Fertilizer Industry Association (IFA), 2014 (<http://www.fertilizer.org>, accessed 18.06.16).
- [6] J.G. Speight, *The Chemistry and Technology of Petroleum*, Fifth ed., Taylor and Francis Group LLC, Boca Raton, c2007.
- [7] J.L. Borges, F.L.P. Pessoa, E.M. Queiroz, Hydrogen source diagram: a procedure for minimization of hydrogen demand in petroleum refineries, *Ind. Eng. Chem. Res.* 51 (2012) 12877–12885.
- [8] L.C. Castañeda, J.A.D. Muñoz, J. Ancheyta, Comparison of approaches to determine hydrogen consumption during catalytic hydrotreating of oil fractions, *Fuel* 90 (2011) 3593–3601.
- [9] Z. Rabei, Hydrogen management in refineries, *Pet. Coal* 54 (4) (2012) 357–368.
- [10] L. Pérez-Moreno, J. Soler, J. Herguido, M. Menéndez, Stable hydrogen production by methane steam reforming in a two zone fluidized bed reactor: experimental assessment, *J. Power Sources* 243 (2013) 233–241.
- [11] H. Shu-Ren, Hydrocarbon steam reforming process: feedstock and catalysts for hydrogen production in China, *Int. J. Hydrog. Energy* 23 (1998) 315–319.
- [12] E. Turpeinen, R. Raudaskoski, E. Pongrácz, R.L. Keiski, Thermodynamic analysis of conversion of alternative hydrocarbon-based feedstocks to hydrogen, *Int. J. Hydrog. Energy* 33 (2008) 6635–6643.

- [13] S.L. Peng, Banking on U.S. shale gas boom, Asia petrochemical firms switch to LPG, <http://www.reuters.com/article/2014/2008/2021/us-asia-lpg-idUSKBN2010GL2012AD20140821> 2014 (accessed 01.10.14).
- [14] F. Beyer, J. Brightling, P. Femell, C. Foster, Steam reforming-50 years of developments and the challenges for the next 50 years, http://www.uhde-ftp.de/cgi-bin/byteserver.pl/archive/upload/uhde_publications_pdf_en_53.00.pdf 2005 (accessed 18.06.16).
- [15] Anon, Shale gas production in the United States from 1999 to 2015 (in trillion cubic feet), <http://www.statista.com/statistics/183740/shale-gas-production-in-the-united-states-since-181999/> 2015 (accessed 23.05.15).
- [16] PPI Energy, Chemicals Team, The effects of shale gas production on natural gas prices, <http://www.bls.gov/opub/btn/volume-2/the-effects-of-shale-gas-production-on-natural-gas-prices.htm> 2013 (accessed 29.11.13).
- [17] R.V. Kumar, R.K. Lyon, J.A. Cole, Unmixed Reforming: A Novel Autothermal Cyclic Steam Reforming Process, Springer, US, 2002.
- [18] M. Ryden, P. Ramos, H₂ production with CO₂ capture by sorption enhanced chemical-looping reforming using NiO as oxygen carrier and CaO as CO₂ sorbent, *Fuel Process. Technol.* 96 (2012) 27–36.
- [19] A. Antzara, E. Heracleous, D.B. Bukur, A.A. Lemonidou, Thermodynamic analysis of hydrogen production via chemical looping steam methane reforming coupled with in situ CO₂ capture, *Int. J. Greenhouse Gas Control* 32 (2015) 115–128.
- [20] V. Dupont, M.V. Twigg, A.N. Rollinson, J.M. Jones, Thermodynamics of hydrogen production from urea by steam reforming with and without in situ carbon dioxide sorption, *Int. J. Hydrog. Energy* 38 (2013) 10260–10269.
- [21] R.K. Lyon, J.A. Cole, Unmixed combustion: an alternative to fire, *Combust. Flame* 121 (2000) 249–261.
- [22] P. Pimenidou, G. Rickett, V. Dupont, M.V. Twigg, High purity H₂ by sorption-enhanced chemical looping reforming of waste cooking oil in a packed bed reactor, *Bioresour. Technol.* 101 (2010) 9279–9286.
- [23] X. Wang, N. Wang, L. Wang, Hydrogen production by sorption enhanced steam reforming of propane: a thermodynamic investigation, *Int. J. Hydrog. Energy* 36 (2011) 466–472.
- [24] D.M. Anderson, P.A. Kottke, A.G. Fedorov, Thermodynamic analysis of hydrogen production via sorption-enhanced steam methane reforming in a new class of variable volume batch-membrane reactor, *Int. J. Hydrog. Energy* 39 (2014) 17985–17997.
- [25] M.V. Kathe, A. Empfield, J. Na, E. Blair, L.-S. Fan, Hydrogen production from natural gas using an iron-based chemical looping technology: thermodynamic simulations and process system analysis, *Appl. Energy* 165 (2016) 183–201.
- [26] A. Hafizi, M.R. Rahimpour, S. Hassanajili, Hydrogen production via chemical looping steam methane reforming process: effect of cerium and calcium promoters on the performance of Fe₂O₃/Al₂O₃ oxygen carrier, *Appl. Energy* 165 (2016) 685–694.
- [27] A. Hafizi, M.R. Rahimpour, S. Hassanajili, High purity hydrogen production via sorption enhanced chemical looping reforming: application of 22Fe₂O₃/MgAl₂O₄ and 22Fe₂O₃/Al₂O₃ as oxygen carriers and cerium promoted CaO as CO₂ sorbent, *Appl. Energy* 169 (2016) 629–641.
- [28] G. Grasa, B. González, M. Alonso, J.C. Abanades, Comparison of CaO-based synthetic CO₂ sorbents under realistic calcination conditions, *Energy Fuel* 21 (2007) 3560–3562.
- [29] S. Mokhtab, W.A. Poe, Handbook of Natural Gas Transmission and Processing, second ed. Gulf Professional Publishing, USA, 2012.
- [30] J.A. Sonibare, F.A. Akeredolu, A theoretical prediction of non-methane gaseous emissions from natural gas combustion, *Energy Policy* 32 (2004) 1653–1665.
- [31] M.W.H. Peebles, Natural Gas Fundamentals, Shell International Gas Limited, London, 1992.
- [32] J.R. Rostrup-Nielsen, J. Sehested, J.K. Nørskov, Hydrogen and synthesis gas by steam and CO₂ reforming, *Adv. Catal.* 47 (2000) 65–137.
- [33] A.P. Simpson, A.E. Lutz, Exergy analysis of hydrogen production via steam methane reforming, *Int. J. Hydrog. Energy* 32 (2007) 4811–4820.
- [34] M.A. Rosen, Thermodynamic investigation of hydrogen production by steam-methane reforming, *Int. J. Hydrog. Energy* 16 (1991) 207–217.
- [35] R.C. Pasel, A. Samsun, R. Tschauder, D. Peters, Stolten, A novel reactor type for autothermal reforming of diesel fuel and kerosene, *Appl. Energy* 150 (2015) 176–184.
- [36] A.M. Adris, B.B. Pruden, C.J. Lim, J.R. Grace, On the reported attempts to radically improve the performance of the steam methane reforming reactor, *Can. J. Chem. Eng.* 74 (1996) 177–186.
- [37] J.R. Fernández, J.C. Abanades, R. Murillo, G. Grasa, Conceptual design of a hydrogen production process from natural gas with CO₂ capture using a Ca–Cu chemical loop, *Int. J. Greenhouse Gas Control* 6 (2012) 126–141.
- [38] N. Patel, B. Baade, V. Khurana, Creating Value through Refinery Hydrogen Management, Asian Refinery Technology Conference Singapore, 2006.
- [39] G. Lee, J. Yu, S.V. Golikeri, B. Klein, Market conditions encourage refiners to recover by-product gases, <http://www.ogi.com/articles/print/volume-111/issue-110/processing/market-conditions-encourage-refiners-to-recover.html> 2013 (accessed 10.12.13).
- [40] Ö. Yildirim, A.A. Kiss, N. Hüser, K. Leßmann, E.Y. Kenig, Reactive absorption in chemical process industry: a review on current activities, *Chem. Eng. J.* 213 (2012) 371–391.
- [41] S.O. Storset, A. Brunsvold, K. Jordal, O. Langorge, R. Anantharaman, D. Berstad, M. Ditaranto, J. Bakkan, R. Blom, T. Peters, K.A. Hoff, P.P. Henriksen, M.L. Fontaine, Technology Survey and Assessment for Piloting of CO₂ Capture Technologies, SINTEF Energy Reserch, Gas Technology, 2013.
- [42] R. Williams, Hydrogen production, <http://www.google.com/patents/US19382021933> (accessed 12.06.15).
- [43] J.R. Hufton, S. Mayorga, S. Siricar, Sorption enhanced reaction process for hydrogen production, *AIChE J.* 45 (1999) 248–256.
- [44] E. Ochoa-Fernandez, G. Haugen, T. Zhao, M. Ronning, I. Aartun, B. Borresen, E. Rytter, M. Ronnekleiv, D. Chen, Process design simulation of H₂ production by sorption enhanced steam methane reforming: evaluation of potential CO₂ acceptors, *Green Chem.* 9 (2007) 654–662.
- [45] R. Chaubey, S. Sahu, O.O. James, S. Maity, A review on development of industrial processes and emerging techniques for production of hydrogen from renewable and sustainable sources, *Renew. Sust. Energy. Rev.* 23 (2013) 443–462.
- [46] A.L. García-Lario, G.S. Grasa, R. Murillo, Performance of a combined CaO-based sorbent and catalyst on H₂ production, via sorption enhanced methane steam reforming, *Chem. Eng. J.* 264 (2015) 697–705.
- [47] A. Brun-tsekhovoi, A. Zadorin, Y.R. Katsobashvili, S. Kourdyumov, The process of catalytic steam-reforming of hydrocarbons in the presence of carbon dioxide acceptor, *Hydrogen Energy Progress VII, Proceedings of the 7th World Hydrogen Energy Conference 1988*, pp. 25–29.
- [48] R. Wess, F. Nores-Pondal, M. Laborde, P. Giunta, Single stage H₂ production, purification and heat supply by means of Sorption-enhanced Steam Reforming of Glycerol. A thermodynamic analysis, *Chem. Eng. Sci.* 134 (2015) 86–95.
- [49] C. Pfeifer, T. Proly, H. Hofbauer, H. Hofbauer, H₂-rich syngas from renewable sources by dual fluidized bed steam gasification of solid biomass, The 12th International Conference on Fluidization - New Horizons in Fluidization Engineering May 13–17, 2007, p. 2007.
- [50] N.B. Rasmussen, Technologies relevant for gasification and methanation in Denmark: detailed analysis of bio-SNG technologies and other RE-gases, http://www.dgc.eu/sites/default/files/flarkiv/documents/R1207_gasification_methanisation.pdf 2012 (accessed 10.05.16).
- [51] D. Schweitzer, M. Beirrow, A. Gredinger, N. Armbrust, G. Waizmann, H. Dieter, G. Scheffknecht, Pilot-scale demonstration of oxy-SER steam gasification: production of syngas with pre-combustion CO₂ capture, *Energy Procedia* 86 (2016) 56–68.
- [52] P. Fu, W. Yi, Z. Li, Y. Li, J. Wang, X. Bai, Comparative analysis on sorption enhanced steam reforming and conventional steam reforming of hydroxyacetone for hydrogen production: thermodynamic modeling, *Int. J. Hydrog. Energy* 38 (2013) 11893–11901.
- [53] R.M. Zin, A. Lea-Langton, V. Dupont, M.V. Twigg, High hydrogen yield and purity from palm empty fruit bunch and pine pyrolysis oils, *Int. J. Hydrog. Energy* 37 (2012) 10627–10638.
- [54] D.E. Ridler, M.V. Twigg, Catalyst handbook, in: M.V. Twigg (Ed.), Steam Reforming, Manson Publishing, London 1996, pp. 225–280.
- [55] M.M. Hossain, H.I. de Lasa, Chemical-looping combustion (CLC) for inherent separations—a review, *Chem. Eng. Sci.* 63 (2008) 4433–4451.
- [56] J. Adanez, A. Abad, F. Garcia-Labiano, P. Gayán, L.F.d. Diego, Progress in Chemical-Looping Combustion and Reforming technologies, *Prog. Energy Combust.* 38 (2012) 215–282.
- [57] C. Linderholm, T. Mattisson, A. Lyngfelt, Long-term integrity testing of spraydried particles in a 10-kW chemical-looping combustor using natural gas as fuel, *Fuel* 88 (2009) 2083–2096.
- [58] M. Källén, M. Rydén, A. Lyngfelt, T. Mattisson, Chemical-looping combustion using combined iron/manganese/silicon oxygen carriers, *Appl. Energy* 157 (2015) 330–337.
- [59] T. Mattisson, A. Järnäs, A. Lyngfelt, Reactivity of some metal oxides supported on alumina with alternating methane and oxygens application for chemical-looping combustion, *Energy Fuel* 17 (2003) 643–651.
- [60] J. Adánez, L.F. de Diego, F. García-Labiano, P. Gayán, A. Abad, Selection of oxygen carriers for chemical-looping combustion, *Energy Fuel* 18 (2004) 371–377.
- [61] A. Lyngfelt, B. Leckner, T. Mattisson, A fluidized-bed combustion process with inherent CO₂ separation; application of chemical-looping combustion, *Chem. Eng. Sci.* 56 (2001) 3101–3113.
- [62] B.J. McBride, S. Gordon, M. Reno, Coefficients of calculating thermodynamics and transport properties of individual species, NASA report TM-4513, <http://ntrs.nasa.gov/archive/nasa/casi.ntrs.nasa.gov/19940013151.pdf> 1993 (accessed 20.02.14).
- [63] K. Bullin, P. Krouskop, Composition variety complicates processing plans for US shale gas, www.digitalrefining.com/article/1000568 2008 (accessed 05.05.14).
- [64] N. MacDowell, N. Florin, A. Buchard, J. Hallett, A. Galindo, G. Jackson, C.S. Adjiman, C.K. Williams, N. Shah, P. Fennell, An overview of CO₂ capture technologies, *Energy. Environ. Sci.* 3 (2010) 1645–1669.
- [65] A. Antzara, E. Heracleous, D.B. Bukur, A.A. Lemonidou, Thermodynamic analysis of hydrogen production via chemical looping steam methane reforming coupled with in situ CO₂ capture, *Energy Procedia* 63 (2014) 6576–6589.
- [66] Z. Martunus, A.D. Helwani, J. Wiheeb, M.R. Kim, Othman, Improved carbon dioxide capture using metal reinforced hydrotalcite under wet conditions, *Int. J. Greenhouse Gas Control* 7 (2012) 127–136.
- [67] J.M. Silva, M.A. Soria, L.M. Madeira, Thermodynamic analysis of Glycerol Steam Reforming for hydrogen production with in situ hydrogen and carbon dioxide separation, *J. Power Sources* 273 (2015) 423–430.
- [68] L. Silvester, A. Antzara, G. Boskovic, E. Heracleous, A.A. Lemonidou, D.B. Bukur, NiO supported on Al₂O₃ and ZrO₂ oxygen carriers for chemical looping steam methane reforming, *Int. J. Hydrog. Energy* 40 (2015) 7490–7501.
- [69] L. Zhu, J. Fan, Thermodynamic analysis of H₂ production from CaO sorption-enhanced methane steam reforming thermally coupled with chemical looping combustion as a novel technology, *Int. J. Energy Res.* 39 (2015) 356–369.
- [70] J. Fan, L. Zhu, Performance analysis of a feasible technology for power and high-purity hydrogen production driven by methane fuel, *Appl. Therm. Eng.* 75 (2015) 103–114.
- [71] J.R. Fernandez, J.C. Abanades, G. Grasa, Modeling of sorption enhanced steam methane reforming—part II: simulation within a novel Ca/Cu chemical loop process for hydrogen production, *Chem. Eng. Sci.* 84 (2012) 12–20.
- [72] I. Martínez, M.C. Romano, J.R. Fernández, P. Chiesa, R. Murillo, J.C. Abanades, Process design of a hydrogen production plant from natural gas with CO₂ capture based on a novel Ca/Cu chemical loop, *Appl. Energy* 114 (2014) 192–208.

- [73] M.A. El-Bousiffi, D.J. Gunn, A dynamic study of steam-methane reforming, *Int. J. Heat Mass Transf.* 50 (2007) 723–733.
- [74] F. Cheng, V. Dupont, M.V. Twigg, Temperature-programmed reduction of nickel steam reforming catalyst with glucose, *Appl. Catal. A Gen.* 527 (2016) 1–8.
- [75] P. Fennell, B. Anthony (Eds.), *Calcium and Chemical Looping Technology for Power Generation and Carbon Dioxide (CO₂) Capture*, Elsevier, 2015.
- [76] P.L. Spath, M.K. Mann, *Life Cycle Assessment of Hydrogen Production via Natural Gas Steam Reforming*, NREL/TP-570-27637, National Renewable Energy Laboratory, US, 2001 (http://pordlabs.ucsd.edu/sgille/mae124_s106/27637.pdf, (18.11.16)).
- [77] W.C. Lattin, V.P. Utgikar, Transition to hydrogen economy in the United States: a 2006 status report, *Int. J. Hydrog. Energy* 32 (2007) 3230–3237.
- [78] D.R. Goodman, *Catalyst handbook*, in: M.V. Twigg (Ed.), *Handling and Using Catalysts in the Plant*, Manson Publishing Limited, London 1996, pp. 140–188.
- [79] J.R.R. Nielsen, J. Sehested, J.K. Nørskov, *Adv. Catal.* 47 (2002) 65–139.
- [80] D.P. Harrison, Sorption-enhanced hydrogen production: a review, *Ind. Eng. Chem. Res.* 47 (2008) 6486–6501.
- [81] P.D. Cobden, G.D. Elzinga, S. Booneveld, J.W. Dijkstra, D. Jansen, R.W. van den Brink, Sorption-enhanced steam-methane reforming: CaO–CaCO₃ capture technology, *Energy Procedia* 1 (2009) 733–739.